

杨岳衡, 吴石头, 车旭东等. 2024. 稀有金属矿物微区同位素定年与示踪. 岩石学报, 40(04): 1023 - 1043, doi: 10.18654/1000-0569/2024.04.01

# 稀有金属矿物微区同位素定年与示踪\*

杨岳衡<sup>1</sup> 吴石头<sup>1</sup> 车旭东<sup>2</sup> 杨明<sup>1,3</sup> 黄超<sup>1</sup> 王浩<sup>1</sup> 杨进辉<sup>1</sup> 王汝成<sup>2</sup> 吴福元<sup>1</sup>

YANG YueHeng<sup>1</sup>, WU ShiTou<sup>1</sup>, CHE XuDong<sup>2</sup>, YANG Ming<sup>1,3</sup>, HUANG Chao<sup>1</sup>, WANG Hao<sup>1</sup>, YANG JinHui<sup>1</sup>, WANG RuCheng<sup>2</sup> and Wu FuYuan<sup>1</sup>

1. 中国科学院地质与地球物理研究所, 岩石圈演化国家重点实验室, 北京 100029

2. 南京大学内生金属矿床成矿机制研究国家重点实验室, 南京大学地球科学与工程学院, 南京 210023

3. 浙江大学海南研究院, 三亚 572025

1. State Key Laboratory of Lithospheric Evolution, Institute of Geology and Geophysics, Chinese Academy of Sciences, Beijing 100029, China

2. State Key Laboratory for Mineral Deposits Research, School of Earth Sciences and Engineering, Nanjing University, Nanjing 210023, China

3. Hainan Institute of Zhejiang University, Sanya 572025, China

2023-11-09 收稿, 2024-02-15 改回.

**Yang YH, Wu ST, Che XD, Yang M, Huang C, Wang H, Yang JH, Wang RC and Wu FY. 2024. In-situ isotopic dating and tracing of the rare-metal minerals in ore deposit. Acta Petrologica Sinica, 40 (4): 1023 - 1043, doi: 10.18654/1000-0569/2024.04.01**

**Abstract** As strategic key metal mineral resources, rare metals such as tungsten, tin, niobium, tantalum, lithium, beryllium, rubidium, cesium, zirconium, hafnium and Rare Earth Elements (REEs), have important research significance in the national economy and national security. The *in situ* isotopic dating and tracing of rare metal ore minerals are the most direct means for conducting research on the mineralization of ore deposits, and have unparalleled advantages in bulk analysis. In recent years, the U-Pb dating and Sr-Nd-Hf isotope tracing of rare metal minerals such as tungsten, tin, niobium, tantalum, zirconium and hafnium have developed rapidly, while the Rb-Sr/Lu Hf dating of rare metal minerals such as lithium, beryllium, rubidium, cesium is thriving. This article reviews the main progress in *in situ* U-Pb dating and Sr-Nd-Hf isotope tracing methods for rare metal minerals such as wolframite, scheelite, cassiterite, columbite-group minerals, monazite, xenotime and bastnaesite. It also looks forward to the *in situ* Rb-Sr dating of rare metal minerals such as (iron, cesium) zinnwaldite, lepidolite, pollucite, potassium feldspar (Tianhe stone), as well as xenotime, apatite, allanite, monazite and wolframite of the broad prospects of Lu Hf dating for microanalysis. The conclusions have been recognized as follows: (1) In addition to using high sensitivity of SF-ICP-MS, combined with elemental imaging, U-Pb dating of low U minerals can not only reveal the correlation between trace elements, but also quickly lock in high U/Pb regions, significantly improving the success of U-Pb dating of low U minerals; (2) The *in situ* Hf isotope of columbite-group minerals, and cassiterite can directly trace the source area of rare metal diagenetic minerals in granite pegmatite, and this work urgently needs to be further strengthened; (3) The emergence of collision/reaction ICP-MS has made isotope dating of minerals with high Rb/Sr or high Lu/Hf ratios a reality, and is a new direction for the future development of rare metal for *in situ* geochronology; (4) The establishment and development of techniques and reference materials complement and promote each other, and are also key technical challenges that urgently need to be addressed. Strategic key metals have become a hot topic in the study of mineralization both domestically and internationally. The study of microanalysis isotopic dating and tracing methods for rare metal minerals such as tungsten, tin, niobium, tantalum, lithium, beryllium, rubidium, cesium, zirconium, hafnium and REEs will undoubtedly make academic contributions to the new round of rare metal deposit research in China.

**Key words** Rare metal minerals; Microanalysis; Isotopic dating and tracing; U-Pb/Rb-Sr/Lu-Hf geochronology

**摘要** 作为战略性关键金属矿产资源, 钨、锡、铌、钽、锂、铍、铷、铯、锆、铪、稀土等稀有金属, 在国民经济与国家安全方面

\* 本文受国家重点研发计划项目(2018YFA0702600)、国家自然科学基金项目(42173034)和岩石圈演化国家重点实验室自主项目(SKL-Z202304)联合资助。

第一作者简介: 杨岳衡, 男, 1970年生, 博士, 正高级工程师, 从事激光微区原位等离子质谱同位素地质年代学方法研究, E-mail: yangyueheng@mail.iggcas.ac.cn

有着重要的研究意义。稀有金属矿石矿物微区同位素定年与示踪,是开展稀有金属矿床成矿作用研究的最直接手段,具有整体分析无可比拟的优点。近年来,钨锡铌钽铍钨钨等稀有金属矿物微区 U-Pb 定年与 Sr-Nd-Hf 同位素示踪发展迅速,而铌钽铍钨等稀有金属矿物微区 Rb-Sr/Lu-Hf 定年正蓬勃发展。本文综述了黑钨矿、白钨矿、锡石、铌钽矿(铌钽氧化物类矿物的简称)、独居石、磷钇矿、氟碳铈矿等稀有金属矿物微区 U-Pb 定年与 Sr-Nd-Hf 同位素示踪技术主要进展,展望了锂云母、铁锂云母、铍沸石、钾长石(天河石)等微区 Rb-Sr 定年与磷钇矿、磷灰石、褐帘石、独居石、黑钨矿、白钨矿等微区 Sm-Nd 和 Lu-Hf 定年的广阔前景,获得如下认识:(1)低铀矿物 U-Pb 定年,除了采用高灵敏度磁式等离子质谱外,元素成像技术能很好地揭示微量元素之间相关性,进而快速锁定高 U/Pb 区域,提高低铀矿物 U-Pb 定年成功率;(2)铌钽矿-锡石激光微区 Hf 同位素能够直接示踪花岗岩-伟晶岩稀有金属成岩成矿物质源区,但这方面工作仍需进一步加强;(3)碰撞/反应池等离子质谱的出现,使高 Rb/Sr、Sm/Nd 或高 Lu/Hf 比矿物的同位素定年成为现实,是未来稀有金属激光微区同位素年代学发展的新方向;(4)实验方法研发与标准物质研制相辅相成、相互促进,仍是当前迫切需要解决的关键技术难题。随着战略性关键金属日渐成为国内外成矿作用研究的热点,钨锡铌钽铍钨钨等稀有金属矿物微区同位素定年与示踪方法研究,必将为我国新一轮稀有金属矿床学研究做出应有的学术贡献。

**关键词** 稀有金属;微区分析;同位素定年与示踪;U-Pb/Rb-Sr/Lu-Hf 年代学

**中图分类号** P597; P618.6

稀有金属包括钨、锡、铌、钽、锂、铍、铷、铯、锆、钪、稀土等,是重要的战略性资源。无论从政治还是经济角度,稀有金属都是国际社会关注的焦点与热点。因此,稀有金属矿产资源研究具有重要的战略意义。我国是稀有金属消费大国,也是资源大国。铌钽铍钨钨是我国的稀缺资源,钨锡稀土是我国的优势资源。作为大国博弈的利器,稀缺资源与优势资源的研究意义同等重要(翟明国等, 2019; 许志琴等, 2021)。成矿年代学是矿床学研究的最基本内容,也是矿床学研究的难点,在研究矿床成因、刻画精细成矿过程和矿床的分布规律中发挥了重要作用。相比于其他热液蚀变矿物、岩浆-热液成因副矿物以及矿物流体包裹体等间接定年手段,矿石矿物的年龄更能有效地代表成矿及矿化时间(蒋少涌等, 2021)。

稀有金属矿物通常产于高分异的花岗岩、伟晶岩、碱性岩和碳酸岩中,这些岩石中的锆石多具有极高的铀含量(超过  $10000 \times 10^{-6}$ ),放射性损伤严重,从而使常规使用的锆石 U-Pb 年代学方法难以获得可靠的成岩成矿年龄(吴福元等, 2023)。但是,黑钨矿、白钨矿、锡石、铌钽矿(铌钽氧化物类矿物)等常与花岗岩-伟晶岩共生或伴生,氟碳铈矿与独居石作为主要稀土矿物常产于碳酸岩或碱性岩中,它们都是 U-Pb 定年的理想矿物(Che *et al.*, 2015; Yang *et al.*, 2019, 2020, 2021, 2022a, 2023b)。而富集铌钽铍的锂云母、铁锂云母、绿柱石、钾长石(天河石)和铍沸石等也常见于高分异的花岗-伟晶岩中,它们较高的 Rb 含量使其成为 Rb-Sr 定年的理想对象(Huang *et al.*, 2023)。随着分析技术的发展,矿物微区同位素定年方法已经在地球科学中有着广泛的应用,成为探讨地球演化历史和各类地质过程的重要手段。与传统的微量或单颗粒同位素稀释法(ID)方法相比,微区同位素定年技术(离子探针、激光探针等),不仅能够揭示常规整体分析所掩盖的精细空间变化信息,同时避免了冗长而繁琐的化学处理过程,从而全面推动了同位素定年的快速发展(吴福元等, 2007)。

虽然钨锡铌钽铍钨钨等稀有金属矿物微区 U-Pb 年代学技术发展迅速,且这些方法的成功研发极大地促进了稀有金属矿床的成矿年代学研究,并取得了大量研究成果(蒋少涌等, 2020, 2021; 毛景文等, 2020; 王汝成等, 2020, 2021)。但较相对成熟的锆石等矿物 U-Pb 同位素定年而言,稀有金属矿物同位素定年与示踪还存在不同程度的方法学问题。本文综述了黑钨矿、白钨矿、锡石、铌钽矿、氟碳铈矿等稀有金属矿物微区 U-Pb 定年与 Sr-Nd-Hf 同位素示踪方法进展,展望了锂云母、铁锂云母、绿柱石、天河石、铍沸石等矿物微区 Rb-Sr 同位素定年与磷钇矿、磷灰石、褐帘石、独居石、黑钨矿、白钨矿等微区 Lu-Hf 同位素定年的广阔前景(表 1)。锆石微区 U-Pb 定年与 Hf 同位素测定方法已经非常成熟并应用广泛(吴福元等, 2007; 王浩等, 2022),本文不再赘述。

## 1 黑钨矿微区 U-Pb 定年

尽管 20 世纪 80 年代初,人们就发现黑钨矿中含有一定量的铀,具有 U-Pb 定年的潜力(Swart and Moore, 1982),但是黑钨矿 U-Pb 年代学工作一直进展缓慢。Frei *et al.* (1998)对津巴布韦 RAN 矿床中的黑钨矿开展了 U-Pb 定年研究,尽管该黑钨矿样品的 U 含量较高( $129 \times 10^{-6}$ ),但由于该样品普通铅含量过高,且样品可能受到元古代热液活动的影响,研究未能获得可靠的年龄数据。真正率先成功获得有意义的黑钨矿 U-Pb 年龄的是德国地学研究中心 Rolf L. Romer 团队,他们对美国科罗拉多 Sweet Home Mine 黑钨矿,开展了 ID-TIMS 工作,获得黑钨矿  $^{206}\text{Pb}/^{238}\text{U}$  年龄为  $25.7 \pm 0.3\text{Ma}$ (Romer and Lüders, 2006);随后,他们对德国 Clara Mine (Pfaff *et al.*, 2009)、法国中央地块(Harlaus *et al.*, 2018a, b)以及我国广西五通(Lecumberri-Sanchez *et al.*, 2014)和江西荡坪(Legros *et al.*, 2020)产出的黑钨矿进行了 U-Pb 定年工作,直接限定了钨矿的成矿时代。Yang *et al.* (2020)对相

表 1 常见稀有金属矿物及同位素定年体系和示踪技术

Table 1 Isotope dating and tracing of the common rare-metal minerals

元素	定年	示踪	备注
钨 (W)	黑钨矿 U-Pb, Lu-Hf 白钨矿 U-Pb, Lu-Hf	白钨矿 Sr-Nd 同位素	
锡 (Sn)	锡石 U-Pb	锡石 Hf 同位素	
铌钽 (Nb/Ta)	铌钽矿 U-Pb	铌钽矿 Hf 同位素	
锆铪 (Zr/Hf)	锆石 U-Pb	锆石 Hf 同位素	
锂 (Li)	锂云母 Rb-Sr 铁锂云母 Rb-Sr		Li 同位素
铍 (Be)	绿柱石 Rb-Sr		
铷 (Rb)	黑云母 Rb-Sr 白云母 Rb-Sr 金云母 Rb-Sr 天河石 Rb-Sr		Li 同位素
铯 (Cs)	铯沸石 Rb-Sr		
稀土 (REE)	独居石 U-Th-Pb, Lu-Hf	独居石 Nd 同位素	
	氟碳铈矿 U-Th-Pb, La-Ba	氟碳铈矿 Sr-Nd 同位素	
	磷灰石 U-Pb, Lu-Hf	磷灰石 Sr-Nd-Hf 同位素	
	褐帘石 U-Pb, Lu-Hf	褐帘石 Sr-Nd 同位素	
	钙钛矿 U-Pb	钙钛矿 Sr-Nd 同位素	
	磷钇矿 U-Pb, Sm-Nd, Lu-Hf	磷钇矿 Nd-Hf 同位素	
	石榴石 U-Pb, Sm-Nd, Lu-Hf	石榴石 Nd-Hf 同位素	

对低普通铅黑钨矿展开了 ID-TIMS U-Pb 定年,并试图研发黑钨矿微区 U-Pb 标准物质,也获得成功。

黑钨矿微区 U-Pb 定年方面, Luo *et al.* (2018, 2019) 采用锆石外部标准水蒸气辅助法对来自法国中央地块 LB 和 MTM 两地的黑钨矿样品进行了实验, 获得与 ID-TIMS U-Pb 年龄一致的结果, 并将该方法应用于我国瑶岗仙和漂塘黑钨矿成矿时代研究 (Deng *et al.*, 2019; 罗涛等, 2021)。Tang *et al.* (2020) 进一步研究发现, MTM 黑钨矿颗粒间 U 含量非常不均一, 普通铅变化大, 不适合作为微区 U-Pb 定年主要标准物质。该作者提出使用 NIST 与 MTM 分别校正实际样品  $^{207}\text{Pb}/^{206}\text{Pb}$  和  $^{238}\text{U}/^{206}\text{Pb}$  比, 然后构建 Tera-Wasserburg 图解获得下交点年龄, 并以西华山、漂塘、朗村、沙麦和白干湖等黑钨矿为实例进行了方法检验。Yang *et al.* (2020) 基于研发的低普通铅黑钨矿微区标准物质, 建立了 LA-ICP-MS 的 U-Pb 方法, 理论计算了黑钨矿 U-Pb 体系封闭温度, 表明大多数地质环境中黑钨矿能有效保持封闭, 是理想 U-Pb 定年对象。同时, 他们还探讨了黑钨矿、钨铁矿和钨锰矿之间的基体效应。表 2 和图 1 汇总了已有黑钨矿 U-Pb 年龄的参考标准物质, YGX2113 (瑶岗仙) 和 Sewa 是适合黑钨矿微区 U-Pb 定年的主要标准物质, 其他则适合作为监控标准物质。

## 2 白钨矿微区 U-Pb 定年与 Sr-Nd 同位素测定

白钨矿具有相对较低 U/Pb 比及较高普通铅, 其 U-Pb 年

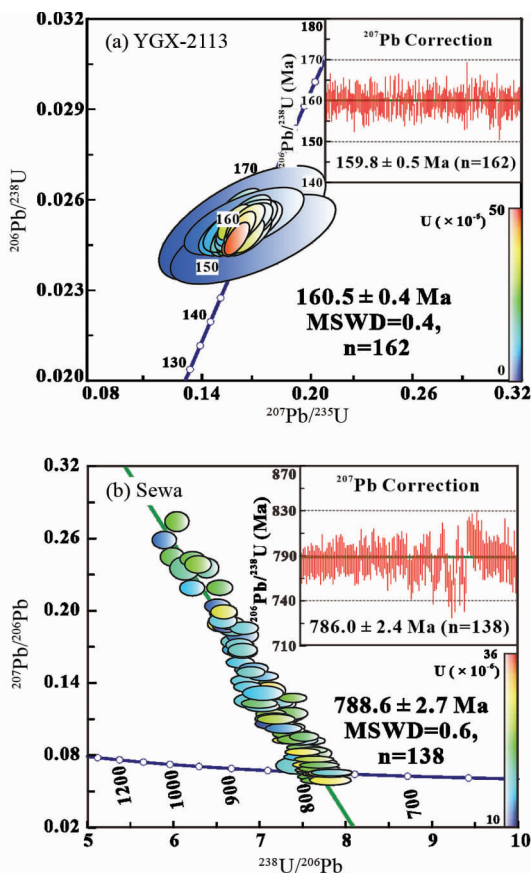


图 1 YGX2113 和 Sewa 黑钨矿激光 U-Pb 年龄

Fig. 1 *In situ* U-Pb age of YGX2113 and Sewa wolframite using laser sampling

龄极少报道。Wintzer *et al.* (2016, 2022) 对美国著名 Yellow Pine 铋金钨矿进行了白钨矿 U-Pb 定年, 得出两组有差别的年龄。ID-TIMS 给出的较老白钨矿 U-Pb 年龄为  $57.52 \pm 0.22\text{Ma}$  和  $56.62 \pm 0.16\text{Ma}$ , 与 Yellow Pine 和 Hangar Flats 中的 adularia 的  $^{40}\text{Ar}/^{39}\text{Ar}$  年龄 ( $56.9 \pm 1.2\text{Ma} \sim 56.38 \pm 0.54\text{Ma}$ ) 一致。与辉铋矿共生的白钨矿年龄则相对年轻 ( $47.4 \pm 1.1\text{Ma}$ ), 但该结果与邻近 Thunder Mountain 的浅热液金银矿床中的 adularia 的  $^{40}\text{Ar}/^{39}\text{Ar}$  年龄 ( $46.00 \pm 0.40\text{Ma}$ ) 一致。因此, 这项研究表明, 钨矿化主要发生在  $\sim 57\text{Ma}$ , 而铋矿化发生  $\sim 47\text{Ma}$ , 首次为 Yellow Pine 铋和钨矿化提供了年龄制约。这是首次成功报道的白钨矿 U-Pb 年龄, 且由于该样品 U 含量较高, 普通铅低, 作者认为该样品可以作为白钨矿激光原位 U-Pb 定年的主要参考标准物质 (表 2)。

法国比利牛斯山脉萨拉乌矿床存在两类与花岗闪长岩侵入体密切相关的钨矿化, 两种矿化的白钨矿和磷灰石在稀土元素含量上存在显著差异, 表明它们源自不同的流体 (Poitrenaud *et al.*, 2020)。锆石、磷灰石和细粒白钨矿 U-Pb 年龄表明, 岩浆锆石和磷灰石形成于  $295 \pm 2\text{Ma}$ , 是在花岗闪长岩侵入体侵位和冷却过程中形成的。粗粒白钨矿的年龄为  $284 \pm 11\text{Ma}$ , 虽不太精确, 但与热液磷灰石的年龄一致

表2 黑钨矿和白钨矿微区 U-Pb 定年参考标准物质

Table 2 U-Pb dating reference materials of wolframite and scheelite for microanalysis

标样名	铀含量 ( $\times 10^{-6}$ )	U-Pb 年龄 (Ma)	方法	$f_{206}$ (%)	参考文献
Sewa	7 ~ 12	789.1 $\pm$ 9.5	ID-TIMS		Yang <i>et al.</i> , 2020
	10 ~ 35	788.6 $\pm$ 2.7	LA-ICP-MS	<7	
MTM	6 ~ 68	334.4 $\pm$ 1.7	ID-TIMS		Harlaux <i>et al.</i> , 2018a
	15 ~ 45	316.5 $\pm$ 5.3	LA-ICP-MS	>20	Carr <i>et al.</i> , 2021
YGX-2113	20 ~ 38	160.9 $\pm$ 0.7	ID-TIMS		Yang <i>et al.</i> , 2020
	5 ~ 50	160.5 $\pm$ 0.4	LA-ICP-MS		
YGX-2107	16 ~ 21	160.1 $\pm$ 1.1	ID-TIMS		Yang <i>et al.</i> , 2020
NM	12 ~ 136	142.3 $\pm$ 1.3	LA-ICP-MS		Tang <i>et al.</i> , 2020
SHM	6 ~ 30	25.7 $\pm$ 0.1	ID-TIMS		Romer and Lüders, 2006
	15 ~ 90	25.6 $\pm$ 0.6	LA-ICP-MS	<3	Yang <i>et al.</i> , 2020
Yellow Pine *		57.52 $\pm$ 0.22	ID-TIMS		Wintzer <i>et al.</i> , 2022
		57.53 $\pm$ 0.25	ID-TIMS		
	3 ~ 32	56.4 $\pm$ 2.6	LA-ICP-MS	1 ~ 17	
	8 ~ 27	57.8 $\pm$ 0.8	LA-ICP-MS	1 ~ 3	
Sch-IGG *	7 ~ 25	51.3 $\pm$ 3.7	LA-ICP-MS	43 ~ 49	本文
WX27 *	3.4 ~ 22.6	141.3 $\pm$ 3.3	LA-ICP-MS	2 ~ 40	Tang <i>et al.</i> , 2022
ZS-Sch-1 *	22 ~ 104	227.1 $\pm$ 3.6	LA-ICP-MS	2 ~ 46	Li <i>et al.</i> , 2023
	7 ~ 184	227.0 $\pm$ 2.2	LA-ICP-MS	0 ~ 34	Wu <i>et al.</i> , 2023

注: \* 为白钨矿, 其他为黑钨矿

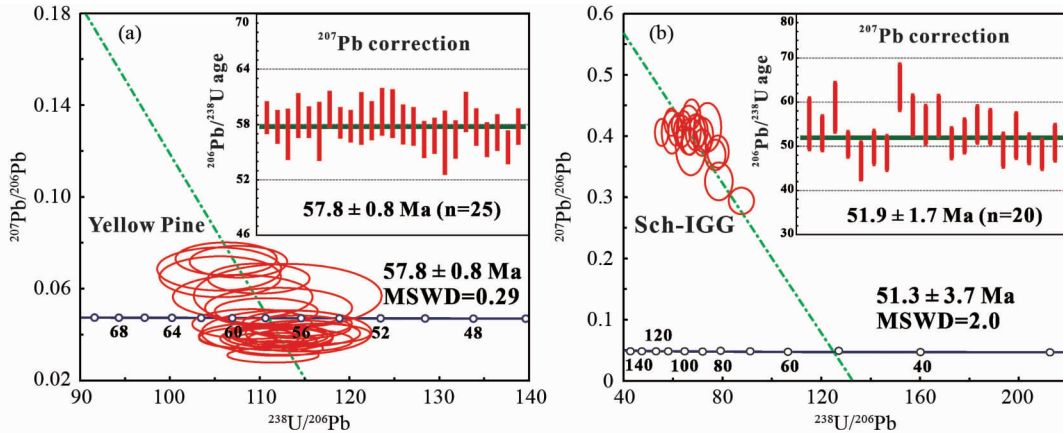


图2 Yellow Pine 和 Sch-IGG 白钨矿激光 U-Pb 年龄

Fig. 2 *In situ* U-Pb age of Yellow Pine and Sch-IGG scheelite using laser sampling

(289  $\pm$  2Ma)。Tang *et al.* (2022) 采用黑钨矿为外标, 进行了白钨矿激光 U-Pb 定年, 显示白钨矿和黑钨矿之间的基体效应并不明显。作者还比较了联合校正法(即 NIST612 校  $^{207}\text{Pb}/^{206}\text{Pb}$ , 而黑钨矿 YGX 校  $^{238}\text{U}/^{206}\text{Pb}$ ) 和黑钨矿标准校正法, 发现两种方法获得的白钨矿年龄一致。将该方法应用于沃溪、白干湖、香炉山、阳储岭和罗维等矿床(时代为 92 ~ 430Ma), 所获得的白钨矿 U-Pb 年龄与前人报道的其他矿物 U-Pb 年龄一致。他们还发现, 沃溪白钨矿 WX27 具有相对高 U ( $\sim 7.1 \times 10^{-6}$ )、低 Pb ( $\sim 0.3 \times 10^{-6}$ ) 特征, 适合做白钨矿微区 U-Pb 定年监控标准物质(表 2)。Li *et al.* (2023) 利用内部标准(ZS-Sch-1, 228  $\pm$  2Ma, 表 2) 测定荞麦山和柿竹园白

钨矿, 并得到石榴石和磷灰石 U-Pb 结果的支持; 作者同时还发现, 氧逸度条件的变化可能是控制白钨矿 U 含量的主要因素(Wu *et al.*, 2023)。图 2 是我们实验室白钨矿激光微区 U-Pb 定年结果, Yellow Pine 由 Wintzer 提供, 另一个是实验室内部标准物质。

白钨矿通常贫 Rb、富 Sr, 富集一定量的稀土, 具有较高 Sm/Nd, 适合开展激光 Sr-Nd 同位素测定, 可以示踪钨成矿物质源区。例如安徽高家垅钨矿, 它由中心斑岩型白钨矿向外过渡为矽卡岩白钨矿和围岩地层中脉状白钨矿, 其 Sr 同位素亦呈逐渐降低趋势, 反映了地层围岩 Sr 同位素的逐渐混染过程(Song *et al.*, 2019)。Li *et al.* (2018) 建立了飞秒激光

多接收等离子质谱白钨矿 Sr 同位素测定方法,研发了白钨矿 Sr 同位素微区标准物质(XJSW 和 HTPW),并开展了相关应用研究(王忠强等, 2020; Li *et al.*, 2021; 王辉等, 2021)。由于标准物质的缺乏,部分实验室目前采用磷灰石(Kozlik *et al.*, 2016; Song *et al.*, 2019; Cao *et al.*, 2020; Han *et al.*, 2020)或玄武岩玻璃(Scanlan *et al.*, 2018)来监控实际样品激光 Sr 同位素测试。

### 3 锡石微区 U-Pb 定年与 Hf 同位素测定

20 世纪 80 年代初,Swart and Moore(1982)对英国西南部著名钨锡矿 Cornwall 中锡石研究表明,锡石富含铀,是 U-Pb 定年的潜在对象。Marini and Botelho(1986)首次利用锡石 U-Pb/Pb-Pb 体系实际测定了锡矿的形成时间,随后得到学者关注。Gulson and Jones(1992)首次成功利用 ID-TIMS 获得南非 Bushveld 杂岩体中与花岗岩有关的 Zaaipplaats 和东南亚锡矿带印度尼西亚 Belitung Island 锡矿床的锡石 U-Pb 年龄,为直接测定锡矿成矿时代提供了一种新途径。McNaughton *et al.*(1993)讨论了 Zaaipplaats 锡矿测年结果的合理性,显示了锡石 U-Pb 年龄在锡矿直接定年的巨大潜力与应用前景。但是,由于在 ID-TIMS U-Pb 实验过程中,锡石很难完全溶解(Gulson and Jones, 1992),ID-TIMS 锡石 U-Pb 方法并没有得到广泛的推广与应用,停滞了十余年之久。可喜的是,我国学者也敏锐意识到锡石 U-Pb 定年的重要意义。刘玉平等(2007)在国内首次利用 ID-TIMS 获得我国最大的锡石硫化物矿床之一的都龙锡锌矿的锡石 U-Pb 年龄,该结果与该地区隐伏花岗岩的锆石 U-Pb 年龄基本一致,表明锡(铜)矿化主要与晚白垩世岩浆热液活动有关。Yuan *et al.*(2008)利用该技术获得我国湖南香花岭锡矿的锡石 U-Pb 年龄与云母 Ar-Ar 年龄基本一致。张东亮等(2011)则从扩散动力学角度对锡石 U-Pb 体系的封闭性进行研究,认为锡石 U-Pb 封闭温度比较高,在大多数地质条件下其同位素体系容易保持封闭状态,这无疑为锡石 U-Pb 年龄直接代表锡矿形成时代提供了理论支持。Neymark *et al.*(2021)发现了继承锡石,为锡石 U-Pb 体系封闭温度较高提供了现实依据。

ID-TIMS 锡石 U-Pb 技术最大的困难是锡石很难完全溶解,这是锡石 ID-TIMS 应用广泛受限的根本原因。近年来,锡石完全溶解技术取得了实质性的进展。如 Carr *et al.*(2020)用 HBr 能够完全溶解锡石,且实验本底非常低。运用该方法,作者对澳洲锡石 Yankee 和我国广泛使用的锡石微区标准物质 AY-4 进行了测定。同样采用 HBr 溶解法,Tapster and Bright(2020)对英国西南部 Cornwall 的 Cligga Head、俄罗斯 SPG 4 和我国江西某地 Jian-1 进行了系统的锡石 ID-TIMS U-Pb 定年。Rizvanova and Kuznetsov(2020)则用浓盐酸完全溶解锡石,获得俄罗斯 SPG II 锡石 U-Pb 年龄结果,该结果与英国地质调查局的测试结果在误差范围内基本一致。Yang *et al.*(2022a)采用 HBr 溶样技术,对普通铅含量较低的锡石样品进

行了 ID-TIMS 分析,研发了 4 个新的锡石微区 U-Pb 标准物质(图 3)。因此,锡石溶解问题目前已基本得到解决,为锡石微区标准物质的 U-Pb 年龄定值提供了便利条件。

相对 ID-TIMS 方法而言,微区 U-Pb 技术具有样品制备简单、分析高效快速、较高空间分辨率等明显优势,同时也避免了锡石难以完全溶解的难题。Yuan *et al.*(2011)首次利用激光联机 Neptune MC-ICP-MS,获得我国湖南芙蓉矿田安源锡矿的锡石 U-Pb 等时线年龄,并且研发了首个锡石微区 U-Pb 定年标准物质(AY-4)。此后 AY-4 作为微区锡石唯一标准物质得到广泛应用,使得我国诸多研究机构现在都能够进行锡石激光 U-Pb 定年(Li *et al.*, 2021; 陈靖等, 2021; Yang *et al.*, 2022a)。与此同时,我国学者还对该锡石样品的封闭温度、化学溶解、普通铅校正、钨氧化物干扰、AY-4 均匀性都进行了深入研究(Yuan *et al.*, 2008, 2011; Zhang *et al.*, 2014; Li *et al.*, 2016; 郝爽等, 2016; 涂家润等, 2016, 2019; 崔玉荣等, 2017; Deng *et al.*, 2018a, b)。从这一点说,我国相关研究机构在锡石微区 U-Pb 定年方法研发及应用研究方面,做出了实质性的贡献(Zhang *et al.*, 2015, 2017a, b)。

国外微区锡石 U-Pb 定年工作差不多比国内晚了近 10 年。Carr *et al.*(2017)利用离子探针评估了 SHRIMP 仪器在测试锡石 U-Pb 过程中的晶轴效应,获得澳洲锡石 Yankee 与 Eurioiwie 的 U-Pb 年龄,该结果与锡石产地其他矿物年龄基本一致。同时,该作者也对锡石 Elsemore 进行 O 同位素分析,显示了锡石微区氧同位素测定上的潜力。此外,在比较了锡石(SPG、Yankee、Jian)激光微区 U-Pb 定年中分别采用锆石 91500、玻璃 612 和 614 作为校正标准对 U-Pb 定年结果的影响后,他们建议采用基体匹配的标准物质(Carr *et al.*, 2023)。Neymark *et al.*(2018)则报道了一种不需要已知年龄锡石标准物质基体匹配校正的激光原位 LA-ICP-MS U-Pb 定年方法,该方法使用 NIST 612 做外标,对低 Th 含量锡石副标进行分馏校正,获得该锡石的 Pb-Pb 年龄。假设该样品 Pb-Pb 年龄与 U-Pb 年龄一致,则可获得 U-Pb 年龄测试值与真实值之间的分馏系数,利用该系数校正实际锡石样品的同位素分馏,然后可采用 Tera-Wasserburg 图解法获得 U-Pb 年龄。该方法对世界各地典型锡石产地的测定样品结果均与前人其他方法一致,验证了方法的可行性(Neymark, 2018; Neymark *et al.*, 2018; Moscati and Neymark, 2020)。表 3 汇总了已有锡石 U-Pb 年龄的参考标准物质,AY-4、SPG、Jian-1、RG-114、BB#7、19GX、Tabba Tabba 和 SIL-1 都适合作为微区 U-Pb 定年主要标准物质,其他适合作为监控标准物质。

与铌钽矿一样,锡石 Hf 含量也较高( $100 \times 10^{-6} \sim 600 \times 10^{-6}$ ),具有开展微区 Hf 同位素测定的潜力,不失为直接示踪锡矿成矿物质源区的有效手段。Kendall-Langley *et al.*(2020)首次对锡石激光 Hf 同位素进行了尝试,但是没有溶液 Hf 同位素数据的支持与验证。Yang *et al.*(2023a)首次建立了激光锡石 Hf 同位素测定方法,并对锡石 U-Pb 标准物质(Rond-A、RG-114、BB#7、19MP 和 19GX)进行了溶液与激光



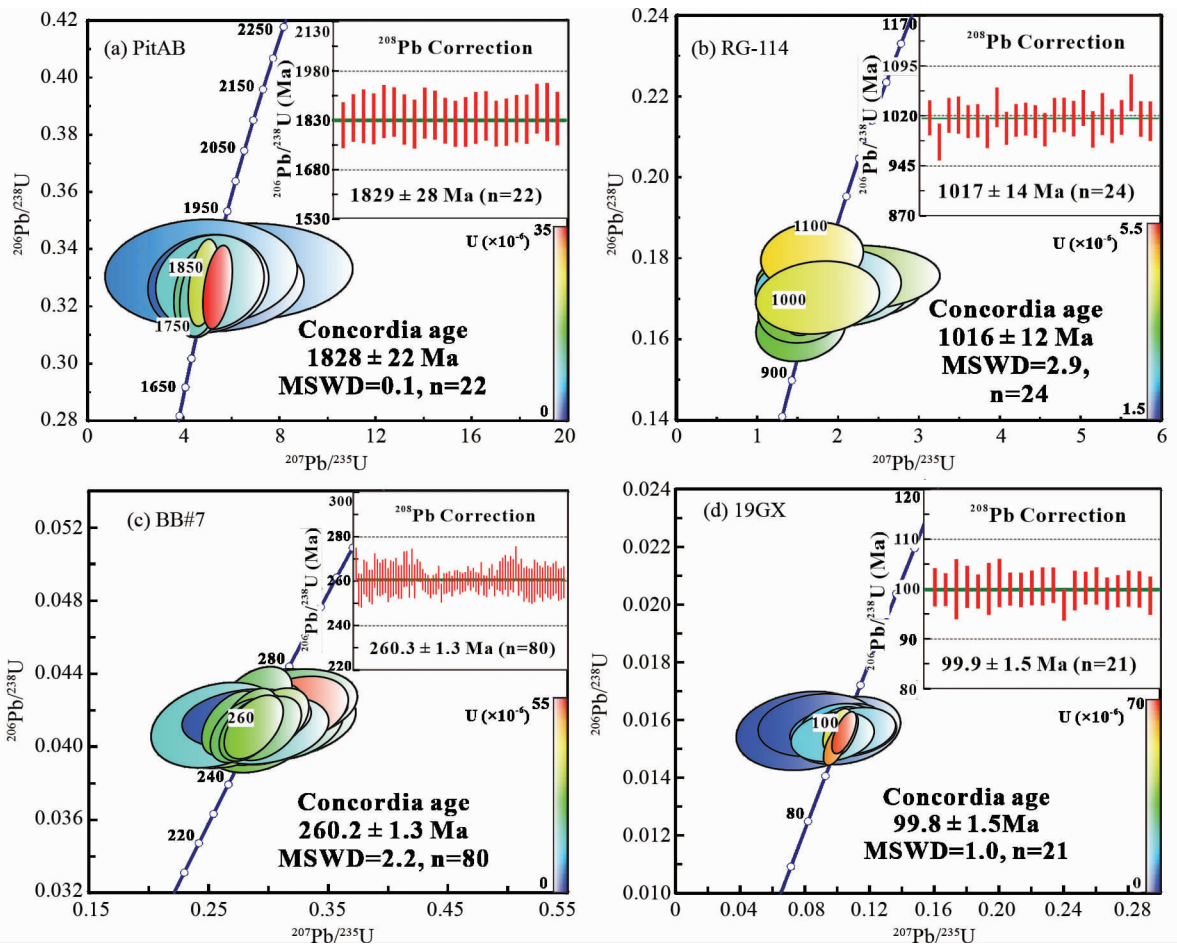


图3 Pit AB、RG-114、BB#7 和 19GX 锡石激光 U-Pb 年龄

Fig. 3 *In situ* U-Pb age of Pit AB, RG-114, BB#7 and 19GX cassiterites using laser sampling

表3 锡石微区 U-Pb 定年参考标准物质

Table 3 U-Pb dating reference materials of cassiterite for microanalysis

标样名	铀含量 ( $\times 10^{-6}$ )	U-Pb 年龄 (Ma)	方法	$f_{206}$ (%)	参考文献
AY-4	30 ~ 33	158.2 $\pm$ 0.4	ID-TIMS		Yuan <i>et al.</i> , 2011
	~ 10	151.9 $\pm$ 2.2	ID-TIMS		Carr <i>et al.</i> , 2020
SPG	10 ~ 72	154.3 $\pm$ 0.7	ID-TIMS		Goodey <i>et al.</i> , 2023
	0 ~ 350	154.5 $\pm$ 1.1	LA-ICP-MS	< 8	Yang <i>et al.</i> , 2022a
	~ 26	1539.5 $\pm$ 0.9	ID-TIMS		Rizvanova and Kuznetsov, 2020
Yankee	5 ~ 27	1536.6 $\pm$ 1.0	ID-TIMS		Tapster and Bright, 2020
	0 ~ 120	1542.7 $\pm$ 1.5	LA-ICP-MS		Neymark <i>et al.</i> , 2018
Jian-1	242.9 $\pm$ 4.8	242.9 $\pm$ 4.8	SIMS	< 18	Carr <i>et al.</i> , 2017
	7 ~ 12	246.5 $\pm$ 0.5	ID-TIMS		Carr <i>et al.</i> , 2020
Cligga Head (Cornwall)	41 ~ 53	156.8 $\pm$ 0.4	LA-ICP-MS		Neymark <i>et al.</i> , 2018
	1 ~ 12	155.0 $\pm$ 0.1	ID-TIMS		Tapster and Bright, 2020
Pit-AB	0 ~ 4	287.9 $\pm$ 2.6	LA-ICP-MS	> 20	Moscato and Neymark, 2020
	0.5 ~ 9	285.1 $\pm$ 0.3	ID-TIMS		Tapster and Bright, 2020
Rond-A	2 ~ 20	1827.8 $\pm$ 6.3	LA-ICP-MS	< 11	Neymark <i>et al.</i> , 2018
	~ 2	1840 $\pm$ 13	ID-TIMS		Yang <i>et al.</i> , 2022a
Rond-A	1.4 ~ 4.2	1012.9 $\pm$ 5.4	LA-ICP-MS	< 10	Neymark <i>et al.</i> , 2018
	~ 2	1022 $\pm$ 5	ID-TIMS		Yang <i>et al.</i> , 2022a

续表 3

Continued Table 3

标样名	铀含量 ( $\times 10^{-6}$ )	U-Pb 年龄 (Ma)	方法	$f_{206}$ (%)	参考文献
RG-114	1.5 ~ 5.5	1015 ± 12	LA-ICP-MS	< 3.6	Yang <i>et al.</i> , 2022a
	~ 1.5	1022 ± 3	ID-TIMS		
BB#7	15 ~ 55	260.2 ± 1.3	LA-ICP-MS	< 2	Yang <i>et al.</i> , 2022a
	7 ~ 22	262.2 ± 0.8	ID-TIMS		
19GX	8 ~ 13	100.3 ± 1.5	LA-ICP-MS	< 4	Yang <i>et al.</i> , 2022a
	8 ~ 13	100.0 ± 0.3	ID-TIMS		
Mt Fransisco	0.6 ~ 14.2	2838 ± 11	LA-ICP-MS		Denholm <i>et al.</i> , 2021
Tabba Tabba	1.8 ~ 6.7	2835 ± 20	LA-ICP-MS		Denholm <i>et al.</i> , 2021
SIL-1		600.9 ± 4.7	ID-TIMS		Liu <i>et al.</i> , 2022
		599.1 ± 4.4	LA-ICP-MS		

Hf 同位素测定,为锡石 Hf 同位素锡矿源区示踪研究提供了新的工具。

#### 4 铌钽矿微区 U-Pb 定年与 Hf 同位素测定

铌钽矿(铌钽氧化物类矿物,包括铌铁矿族矿物(包括铌铁矿、钨锰矿、钽锰矿和钽铁矿)和重钽铁矿两个矿物族的矿物,本文简称铌钽矿),作为主要铌钽金属矿物,通常具有较高 U 含量与低普通铅,是 U-Pb 定年的理想矿物。Aldrich *et al.* (1956)首次采用同位素稀释热电质谱(ID-TIMS)技术对 Brown Derby 伟晶岩中铌钽矿进行 U-Pb 定年,由于大量富铀包裹体、交代环带及其复杂的重结晶结构,其 U-Pb 年龄不谐和,因此铌钽矿 U-Pb 定年三十余年没有显著进展。Romer and Wright(1992)发展了酸化学淋滤法,尽可能去除包裹体,提高了 $^{206}\text{Pb}/^{204}\text{Pb}$ 比,得到了近似谐和的 U-Pb 年龄,表明铌钽矿 U-Pb 定年在过铝质花岗岩、伟晶岩、碱性岩和碳酸岩侵入体中,是一种非常重要定年工具。自此,Romer 及合作者发表了一系列铌钽矿 ID-TIMS 定年工作成果(Romer and Smeds, 1994, 1996, 1997; Romer and Lehmann, 1995; Romer *et al.*, 1996)。

虽然 ID-TIMS 能够给予高精度数据,但涉及繁琐的化学处理过程,且仍无法完全消除富铀包裹体、蜕晶化对测年结果的影响,其 U-Pb 年龄通常不谐和(反向不谐和或铅丢失),微区 U-Pb 定年无疑是最理想的手段。Smith *et al.* (2004)首次采用 266 纳米激光与 VG 公司 Axiom MC-ICP-MS 联机,测定已知铌钽矿 ID-TIMS U-Pb 年龄,获得了可靠的 Pb-Pb 年龄,但其激光 U-Pb 结果与 ID-TIMS 一样不谐和。作者认为,铌钽矿 U-Pb 年龄受到后阶段的扰动重置或蜕晶化的影响不容忽视。但是,由于没有微区铌钽矿标准物质,采用的独居石标准物质也无法有效校正铌钽矿 U/Pb 分馏,其 U-Pb 年龄可靠性值得商榷。除了独居石之外,其他实验室则采用锆石作为标准物质,开展了铌钽矿激光微区 U-Pb 定年诸多应用研究(Dill *et al.*, 2007; Melcher *et al.*, 2008; Dewaele *et al.*,

2011; Melleton *et al.*, 2012; Deng *et al.*, 2013)。

Melcher *et al.* (2015)首次报道了来自马达加斯加 Coltan139 的 ID-TIMS U-Pb 年龄结果。Che *et al.* (2015)详细研究了激光微区 U-Pb 定年中锆石与铌钽矿的基体效应,发现铌钽-铁锰主量元素变化对激光微区 U-Pb 定年影响不显著,建议 Coltan139 作为铌钽矿微区 U-Pb 主要标准物质,此后 Coltan139 一直作为主要的铌钽矿标准物质,广泛应用于激光微区铌钽矿 U-Pb 定年,并取得了大量研究成果(Melcher *et al.*, 2017; Che *et al.*, 2019)。Legros *et al.* (2019)详细研究了铌钽矿主量元素变化对 SIMS U-Pb 定年的影响。他们对 9 个已知 ID-TIMS 的铌钽矿样品,进行了 U-Pb 定年,发现铌钽变化与 $^{206}\text{Pb}/^{238}\text{U}$ 年龄具有很好相关性,而铁锰变化则不明显。最近,新的铌钽矿微区 U-Pb 标准物质也不断推出(Xiang *et al.*, 2023),并对广泛使用的 Coltan139 标准进行了 ID-TIMS U-Pb 年龄的重新检验(Yang *et al.*, 2023b)。表 4 和图 4 汇总了已有铌钽矿 U-Pb 年龄的参考标准物质,Coltan139、CT1、CT3、Buranga、SN3、Rongi 都适合作为微区 U-Pb 定年主要标准物质,而其他则可以作为监控标准物质。

除了 U-Pb 定年外,铌钽矿 Hf 含量较高( $50 \times 10^{-6} \sim 2650 \times 10^{-6}$ ),具有开展微区 Hf 同位素测定的潜力,从而为直接示踪其铌钽矿成矿物质源区提供有效工具(李杨等, 2016; Tang *et al.*, 2021)。Marko *et al.* (2014<sup>①</sup>)简要报道了铌钽矿微钻取样的 Lu-Hf 同位素稀释法结果,其初始 Hf 同位素变化大,其后续工作未见发表。Tang *et al.* (2021)建立了铌钽矿溶液与激光 Hf 同位素测定方法,证明大量钽的存在会严重影响铌钽矿溶液与激光 Hf 同位素测定。为此该作者建立了适合铌钽矿的两阶段化学流程:首先采用 LN 树脂,实现铌钽钪与其他基体元素与干扰元素的分离;然后采用 AG1-X8 树脂,实现铌钽与钪的分离,从而实现了铌钽矿溶液

① Marko L, Gerdes A, Melcher F and van Lichtervelde M. 2014. Presented in part at the 21<sup>st</sup> Meeting of the International Mineralogical Association, 1-5, September, Johannesburg, South Africa

表4 铌钽矿、氟碳铈矿和磷钇矿微区 U-Pb 定年参考标准物质

Table 4 U-Pb dating reference materials of columbite-group minerals (CGM), bastnaesite and xenotime for microanalysis

标样名	U-Pb 年龄 (Ma)	方法	$f_{206}$ (%)	参考文献
Coltan139	506.6 ± 2.4	ID-TIMS		Melcher <i>et al.</i> , 2015
	505.4 ± 1.0	ID-TIMS		
	507.9 ± 1.3	ID-TIMS		Yang <i>et al.</i> , 2023b
	507.9 ± 1.4	LA-ICP-MS	< 8	
Coltan17	~ 502	LA-ICP-MS		Gäbler <i>et al.</i> , 2011
	502.1 ± 2.9	LA-ICP-MS	< 15	Yang <i>et al.</i> , 2023b
CT1	2046.8 ± 1.1	ID-TIMS		Legros <i>et al.</i> , 2019
CT3	2053.2 ± 1.3	ID-TIMS		Legros <i>et al.</i> , 2019
CT4	2044.5 ± 1.6	ID-TIMS		Legros <i>et al.</i> , 2019
Buranga	905.2 ± 2.3	ID-TIMS		Legros <i>et al.</i> , 2019
Rongi	931.5 ± 2.5	ID-TIMS		Legros <i>et al.</i> , 2019
CC1716	326.3 ± 0.6	ID-TIMS		Legros <i>et al.</i> , 2019
NP2	387.1 ± 4.0	LA-ICP-MS		Tang <i>et al.</i> , 2017
	380.3 ± 2.4	ID-TIMS		Legros <i>et al.</i> , 2019
	377.5 ± 3.3	SIMS	< 8	
NT-2	376.0 ± 4.0	LA-ICP-MS		Che <i>et al.</i> , 2015
	372.0 ± 2.3	ID-TIMS		Legros <i>et al.</i> , 2019
	371.3 ± 3.7	SIMS	> 20	
SN3	404.0 ± 1.3	ID-TIMS		Xiang <i>et al.</i> , 2023
HND	136.2 ± 0.9	ID-TIMS		Xiang <i>et al.</i> , 2023
	135.5 ± 0.8	LA-ICP-MS	< 3	
RL2	135.7 ± 0.3	ID-TIMS		Xiang <i>et al.</i> , 2023
	133.3 ± 3.0	LA-ICP-MS	< 2	
DDB	202.0 ± 1.0	ID-TIMS		Yang <i>et al.</i> , 2023b
	202.1 ± 1.0	LA-ICP-MS	< 5	
ZKW	203.0 ± 1.6	ID-TIMS		Yang <i>et al.</i> , 2023b
	202.6 ± 1.0	LA-ICP-MS	< 2	
Xtc*	2572 ± 33	ID-TIMS		Fletcher <i>et al.</i> , 2000
Z6413*	993.8 ± 0.7	ID-TIMS		Stern and Rayner, 2003
	997.9 ± 0.2	ID-TIMS		Schoene <i>et al.</i> , 2006
MG-1*	409.1 ± 1.1	ID-TIMS		Fletcher <i>et al.</i> , 2004
BS-1*	508.8 ± 1.4	ID-TIMS		Fletcher <i>et al.</i> , 2004
XN01*	513.4 ± 0.5	ID-TIMS		Vasconcelos <i>et al.</i> , 2018
XN02*	515.4 ± 0.2	ID-TIMS		Vasconcelos <i>et al.</i> , 2018
K-9 <sup>#</sup>	118 ± 1	ID-TIMS		Sal'Nikova <i>et al.</i> , 2010
	116.80 ± 0.13	ID-TIMS		Li <i>et al.</i> , 2020a
ZK4002-8 <sup>#</sup>	407.8 ± 3.3	ID-TIMS		Qu <i>et al.</i> , 2019

注: \* 为磷钇矿, <sup>#</sup> 为氟碳铈矿, 其他为铌钽矿

Hf 同位素测定。针对铌钽矿激光 Hf 同位素测定难题, 他们发现常规的  $^{179}\text{Hf}/^{177}\text{Hf}$  无法进行质量分馏校正, 为此他们首次提出  $^{178}\text{Hf}/^{177}\text{Hf}$  进行铌钽矿激光 Hf 同位素质量分馏校正, 并得到了溶液方法的验证与支持, 解决了钽强峰拖尾干扰 Hf 同位素测定的难题, 为铌钽金属矿物 Hf 同位素源区示踪开辟了新途径。

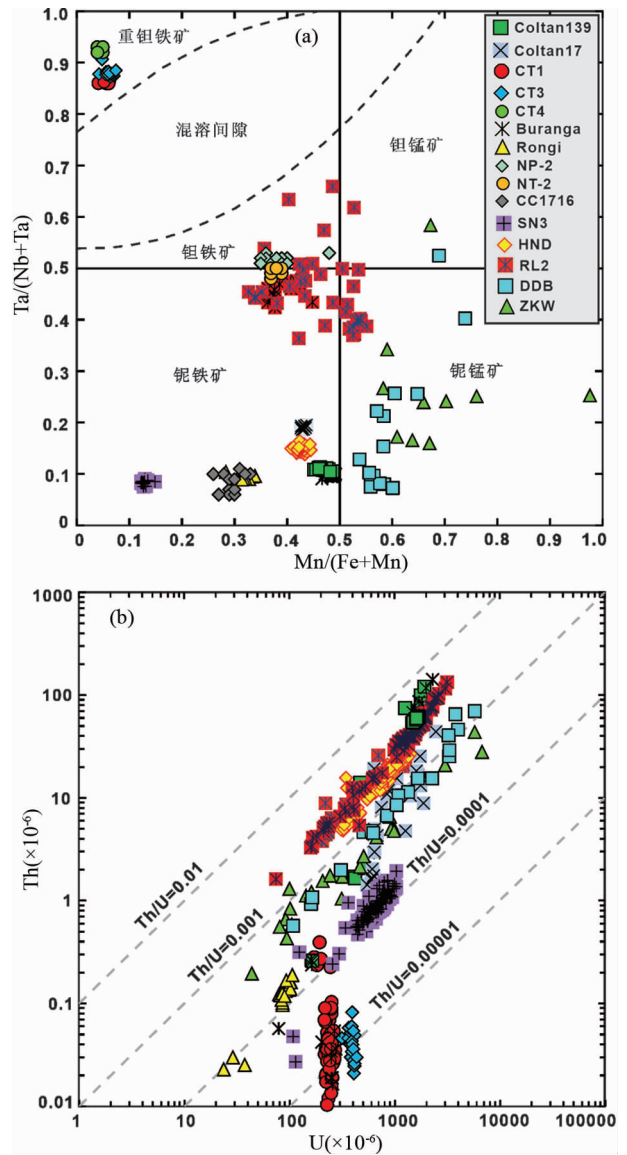


图4 铌钽矿微区 U-Pb 定年参考标准物质的四方图与 U-Th 含量关系图

Fig. 4 The quadrilateral diagram and the Th and U contents of most CGM reference materials for microanalysis

## 5 稀土矿物微区 U-Pb 定年与 Sr-Nd 同位素测定

氟碳铈矿、独居石、磷钇矿、磷灰石和褐帘石等, 作为主要稀土矿物, 是 U-Pb 定年的理想对象。其中独居石与磷钇矿, 大多具有非常低普通铅, 其微区 U-Pb 定年方法非常成熟 (Fletcher *et al.*, 2000, 2004; Stern and Rayner, 2003; Schoene *et al.*, 2006; 刘志超等, 2011; Liu *et al.*, 2012; Li *et al.*, 2013; Ling *et al.*, 2017; Luo *et al.*, 2018; Vasconcelos *et al.*, 2018), 这里不再赘述。氟碳铈矿族矿物属于氟碳酸盐



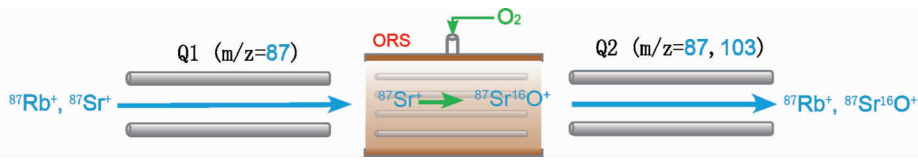


图5 三重四级杆等离子质谱的干扰( $^{87}\text{Rb}$  干扰 $^{87}\text{Sr}$ )消除原理

Fig. 5 The principle of eliminating interference ( $^{87}\text{Rb}$  interference  $^{87}\text{Sr}$ ) in triple quadrupole plasma mass spectrometry

类型,主要包括氟碳铈矿、氟菱钙铈矿、碳氟钙铈矿和氟碳钙铈矿。氟碳铈矿通常具有较高的 U、Th 含量,适合 U-Th-Pb 定年(Sal'Nikova *et al.*, 2010),也适合 La-Ba 定年(Nakai *et al.*, 1988, 1989)。Sal'Nikova *et al.* (2010)首次报道了氟碳铈矿 ID-TIMS U-Pb 定年工作,随后 Yang *et al.* (2014)建立了氟碳铈矿激光 U-Pb 定年方法,发现 K-9 是低普通铅的理想微区标准物质。利用建立的方法,Yang *et al.* (2019)对我国白云鄂博、冕宁-德昌、微山,瑞典 Bastnas,美国 Mountain Pass,俄罗斯图瓦共和国 Karasug,马拉维 Zomba-Malosa 和马达加斯加等稀土矿产出的氟碳铈矿进行 U-Th-Pb 定年和 Sr-Nd 同位素测定,并探讨其成矿时代与物质源区。Ling *et al.* (2016)则建立离子探针 Th-Pb 定年方法,并应用冕宁-德昌稀土矿研究。Qu *et al.* (2019)对北秦岭太平镇稀土矿的氟碳铈矿进行激光微区 U-Pb 定年与 ID-TIMS 测定,直接限定了稀土矿的成矿时代(涂家润等, 2017)。Li *et al.* (2020a)对微区标准物质 K-9 进行了系统 ID-TIMS U-Pb 和 Th-Pb 年龄标定,进一步表征其微区定年标准物质的可靠性。

氟碳铈矿与独居石富集轻稀土,能够进行激光微区 Sr-Nd 同位素测定,从而直接限定碳酸岩、碱性岩及稀土矿床的物质源区。目前,轻稀土富集矿物(独居石、榍石、磷灰石、褐帘石、氟碳铈矿、钙钛矿等)激光微区 Sr-Nd 同位素测定已经成为一种成熟技术(Foster and Vance, 2006; Yang *et al.*, 2008, 2009, 2014, 2019, 2022b; Iizuka *et al.*, 2011; Liu *et al.*, 2012; 侯可军等, 2013; Xu *et al.*, 2015, 2018; Ma *et al.*, 2019; Qu *et al.*, 2019; Altenberger *et al.*, 2022; Lana *et al.*, 2022; Prokopyev *et al.*, 2023),但是,对于重稀土富集矿物(磷钇矿、硅铈钇矿等),目前仅有一篇文献报道(Nazari-Dehkordi *et al.*, 2018)。该作者对澳大利亚北部的热液磷钇矿,开展激光 Sm-Nd 同位素测定,结合激光 U-Pb 年龄显示,初始 Nd 同位素具有非常大的变化范围(-28 ~ -12),由于没有磷钇矿溶液 Sm-Nd 同位素数据的检验,作者只是和全岩初始 Nd 同位素进行比较(-17 ~ -13),让人对磷钇矿激光 Sm-Nd 同位素测定的可靠性产生疑问,毕竟这些磷钇矿具有相同的年龄,理论上,其初始 Nd 同位素应该基本一致,不应该有太大的变化。

## 6 云母与钾长石等矿物微区 Rb-Sr 定年

近十年来,三重四级杆等离子质谱(ICP-MS/MS)的出

现,使得激光微区 Rb-Sr 定年成为现实。安捷伦公司先后推出了 8800(2012)、8900(2016) ICP-MS/MS;热电公司则推出了 iCAP TQ ICP-MS/MS(2017)和 Neoma MC-ICP-MS/MS(2021);珀金埃尔默公司也推出 NexION 5000 ICP-MS/MS(2020)。ICP-MS/MS 与普通 ICP-MS 的本质区别是,在碰撞反应池前添加了一个具有预过滤功能的四级杆,其作用是保证只有相同质量数的离子通过,而其他离子则无法通过四级杆,也就保证了后面的离子反应可控,不引入新的干扰,然后碰撞反应池中的气体发生离子碰撞/反应,实现同质异位素的干扰分离(图 5)。以 Rb-Sr 体系为例, $Q_1$  只让 $^{87}\text{Rb}^+$  和 $^{87}\text{Sr}^+$  通过,在碰撞反应池中 $^{87}\text{Sr}^+$  与反应气(氧气/六氟化硫/一氧化二氮/氟化甲烷)全部反应, $^{87}\text{Rb}^+$  不反应,实时在线实现 $^{87}\text{Rb}^+$  和 $^{87}\text{Sr}^+$  的干扰分离,而以前则需要通过繁琐的离子交换等化学分离才能实现,这是激光微区 Rb-Sr 定年得以实现的基本原理与条件(Zack and Hogmalm, 2016)。

目前已经有白云母、黑云母、金云母、钾长石、海绿石、伊利石等激光微区 Rb-Sr 定年及应用报道(Siebel *et al.*, 2005; Tillberg *et al.*, 2017, 2020; Şengün *et al.*, 2019; Li *et al.*, 2020b; Kendall-Langley *et al.*, 2020; Olierook *et al.*, 2020; Laureijs *et al.*, 2021; Glorie *et al.*, 2022; Gou *et al.*, 2022; Gyomlai *et al.*, 2022; Liebmann *et al.*, 2022; Lihter *et al.*, 2022; Redaa *et al.*, 2022; Scheibelhofer *et al.*, 2022; Simpson *et al.*, 2022, 2023; Subarkah *et al.*, 2022; Cruz-Urbe *et al.*, 2023; Huang *et al.*, 2023; Larson *et al.*, 2023; Kelepilic *et al.*, 2023; Kharkongor *et al.*, 2023; Ribeiro *et al.*, 2023),这些矿物多为主要造岩矿物或稀有金属矿石矿物,在稀有金属产出的花岗岩-伟晶岩也比较常见,无疑它们的激光微区 Rb-Sr 定年具有广阔的应用前景(王汝成等, 2017, 2019; 吴福元等, 2017, 2021, 2023; 秦克章等, 2021; 吴昌志等, 2021; 李建康等, 2023)。

Moens *et al.* (2001)最早利用 Elan 6100 DRC ICP-MS,反应气为氟化甲烷,同时测定 $^{87}\text{Rb}/^{86}\text{Sr}$  与 $^{87}\text{Sr}/^{86}\text{Sr}$ ,尝试溶液全岩 Rb-Sr 定年,获得  $353 \pm 40\text{Ma}$  等时线年龄,尽管该结果与 ID-TIMS 相比有一定差距( $353 \pm 25\text{Ma}$ ),但仍显示出该技术未来的巨大潜力(Bolea-Fernandez *et al.*, 2016a, b, 2017, 2021)。Zack and Hogmalm(2016)首次建立了 8800 ICP-MS/MS 富 Rb 矿物的激光 Rb-Sr 定年方法,系统比较三种反应气(氧气/六氟化硫/一氧化二氮)与 Sr 产物灵敏度,指出对于高 Rb 低 Sr(如云母)矿物,需使用基体匹配的标准物质

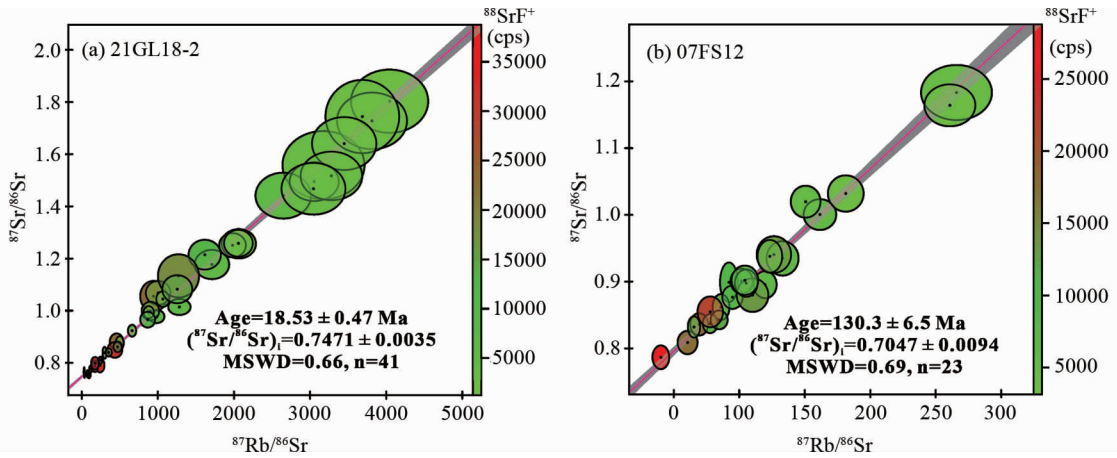


图6 锂云母(a)与黑云母(b)激光微区 Rb-Sr 定年(据黄超等 2023)

Fig. 6 *In situ* Rb-Sr dating of lepidolite and biotite using LA-ICP-MS/MS (after Huang *et al.*, 2023)

(Hogmalm *et al.*, 2017)。对于单点激光 Rb-Sr 模式年龄的可行性,作者认为问题的关键是对初始 $^{87}\text{Sr}/^{86}\text{Sr}$ 的合理估计。作者提出了一系列与地质相关的初始 $^{87}\text{Sr}/^{86}\text{Sr}$ 组成,如地幔源岩浆岩为 $0.703 \pm 0.003$ ,演化岩浆岩为 $0.715 \pm 0.015$ ,地壳岩石为 $0.730 \pm 0.030$ 。结果表明,样品的 $^{87}\text{Sr}/^{86}\text{Sr}$ 反映了单点 Rb-Sr 模式年龄的可靠性。如果地幔源岩浆岩样品的 $^{87}\text{Sr}/^{86}\text{Sr} > 1$ ,地壳岩石样品的 $^{87}\text{Sr}/^{86}\text{Sr} > 4.5$ ,则其模式年龄基本不受初始 $^{87}\text{Sr}/^{86}\text{Sr}$ 的影响。最后,以粉末压片 Mica-Mg 金云母为标准物质,对黑云母(Mount Dromedary, La Posta, McClure Mountain)、白云母(Högsbo)和 Mica-Fe 粉末压片进行了单点 Rb-Sr 定年测试,建议这些样品可以作为激光原位 Rb-Sr 定年监控参考标准物质(Rösel and Zack, 2022),并应用于土耳其西部阿克萨巴德金矿床的白云母、钾长石与断层中的伊利石定年研究。

Jegal *et al.* (2022) 采用 ID-TIMS 对金云母、黑云母、钾长石和海绿石四个粉末参考物质进行标定,给出了 $^{87}\text{Rb}/^{87}\text{Sr}$ 和 $^{87}\text{Sr}/^{86}\text{Sr}$ 比值与年龄参考值,为这些矿物后续激光原位 Rb-Sr 定年提供了基础数据。Gorojovsky and Aland(2020)研究了不同激光与质谱参数、外部标准物质对原位 Rb-Sr 定年的影响,表明激光波长与频率对 $^{87}\text{Rb}/^{86}\text{Sr}$ 和 $^{87}\text{Sr}/^{86}\text{Sr}$ 准确度有显著影响,优化仪器参数可以降低基体效应(Wang *et al.*, 2022)。Redaa *et al.* (2021, 2023) 同样发现激光波长对 Rb-Sr 分馏有显著影响,从而导致基体效应,金云母粉末压片标准物质与天然云母矿物的剥蚀特征和分馏模式相比仍存在差异,认为采用与目标矿物基体匹配的标准物质对进一步提高年龄的准确性至关重要。黄超等(2023)基于 i CAP TQ ICP-MS/MS,提出将黑云母作为基体匹配的第二标准物质,对云母样品进行两步法校正,校正标准玻璃与天然云母样品间的基体效应,提高云母激光原位微区 Rb-Sr 等时线定年的准确度。图 6 是西藏吉隆锂云母和北京房山岩体黑云母的激光原位 Rb-Sr 定年结果,显现了未来锂铍钽稀有金属矿物微区 Rb-Sr 定年的潜在价值与前景。热电公司则先后与

布里斯托大学、芝加哥大学和加州大学等机构合作,一直致力于研发带碰撞反应池的多接收等离子质谱,经历了原型机 Proteus、Vienna 到商业产品 Neoma MC-ICP-MS/MS,其质量预过滤器也经历了从四级杆到磁铁的过程,并应用于地球和地外样品原位 Rb-Sr 定年来检验仪器的性能(Bevan *et al.*, 2021; Craig *et al.*, 2021; Dauphas *et al.*, 2022)。

## 7 磷灰石与磷钇矿等微区 Lu-Hf 定年

与激光微区 Rb-Sr 定年相比,激光微区 Lu-Hf 定年方法则少有报道。Zack and Hogmalm(2015)基于 8800 首次报道了磷钇矿激光微区 Lu-Hf 定年,指明了重稀土富集矿物(硅铍钇矿、易解石、黑稀金矿等)的激光微区 Lu-Hf 定年的广阔前景。Simpson *et al.* (2021) 基于 8900 采用氦气与氦气预混气首次报道了石榴石、磷灰石和磷钇矿的激光微区 Lu-Hf 定年方法,作者发现不同矿物之间激光微区 Lu-Hf 定年的基体效应非常明显。Wu *et al.* (2023) 首次基于 i CAP TQ ICP-MS/MS,采用纯氦气,研发了石榴石、磷灰石和磷钇矿的激光微区 Lu-Hf 定年方法,指出采用同种矿物可以有效消除基体效应,详细评估了 Yb、Lu 与氦气反应产率对不同年龄 Hf 同位素的影响,并比较了 Lu-Hf 定年的等时线年龄与模式年龄(图 7)。激光微区 Lu-Hf 定年有可能在含石榴石样品中获得高空间分辨的 Lu-Hf 年龄,而传统方法很难实现,这为多变质历史的复杂地区的快速年龄普查提供了契机(Brown *et al.*, 2022; Tamblyn *et al.*, 2022)。与磷灰石 U-Pb 体系相比,其 Lu-Hf 体系较高的封闭温度允许高温热历史重建,磷灰石 Lu-Hf 定年允许对低 U 和高 Pb 的样品进行定年。由于磷灰石几乎没有普通铅,从而可以计算单点 Lu-Hf 模式年龄,这为碎屑物源研究打开了新的窗口(Gillespie *et al.*, 2022)。磷钇矿原位 Lu-Hf 定年为其 U-Pb 定年提供了另一种手段,并且可能特别有利于稀土矿床的定年。

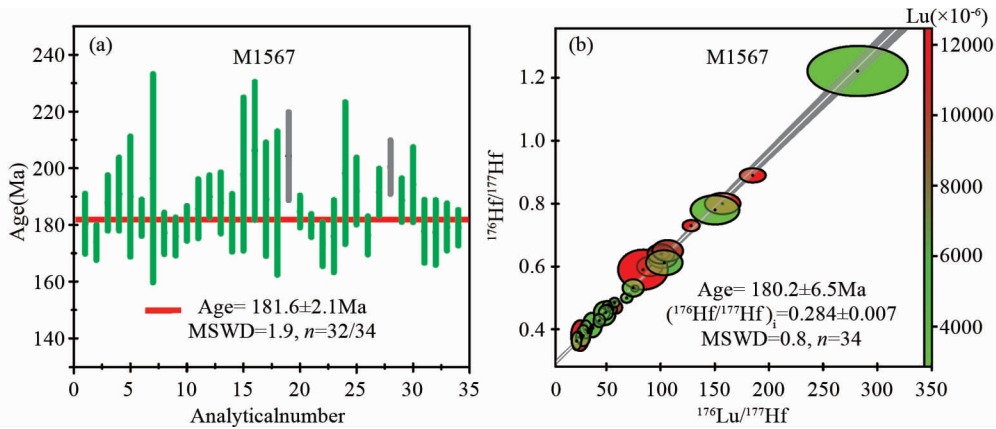


图7 磷钇矿激光 Lu-Hf 模式年龄与等时线年龄

Fig. 7 *In situ* Lu-Hf dating of model and isochronology age for xenotime using LA-ICP-MS/MS

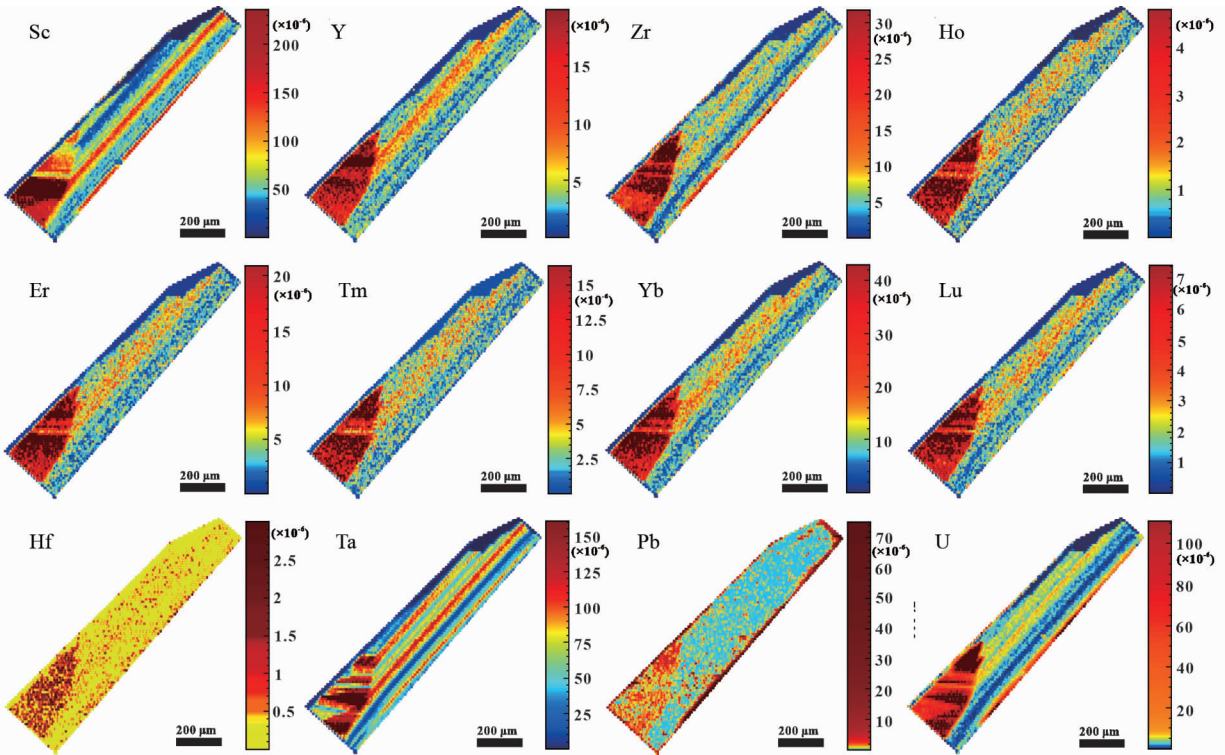


图8 黑钨矿 SHM 激光二维扫描图

Fig. 8 The trace element mapping of SHM wolframite using LA-ICP-MS

## 8 展望与结语

### 8.1 低铀矿物微区 U-Pb 定年与 Sr-Nd-Hf 同位素测定

随着分析技术的快速发展,未被开发的适合 U-Pb 定年矿物越来越少,而绝大多数低铀 U-Pb 定年对象都含有不同程度普通铅,为了提高低铀矿物微区 U-Pb 定年成功率,通常需要高灵敏度的仪器,如扇形磁场 (SF)-ICP-MS 和多接收 (MC)-ICP-MS。目前也有报道采用四级杆 (Q) ICP-MS 进行

低铀矿物 U-Pb 定年,但往往需要较大的激光束斑,这使得空间分辨率变差,因此高灵敏度的 Element XR 或 Neptune Plus MC-ICP-MS,比 Q-ICP-MS 更适合低 U 含量矿物激光微区 U-Pb 定年 (Tang *et al.*, 2020, 2022; Wu *et al.*, 2020; Yang *et al.*, 2020, 2022a; Zhang *et al.*, 2021; Wei *et al.*, 2022; 罗涛和胡兆初, 2022; 吴石头等, 2022; 谢博航等, 2023)。同时,采用激光二维图形技术,是一种比较切实可行的办法,一方面能够很直观揭示不同元素之间的相关性,如黑钨矿铀与重稀土明显相关 (图 8),锡石钛锆钽钨钨相关性 (图 9),另



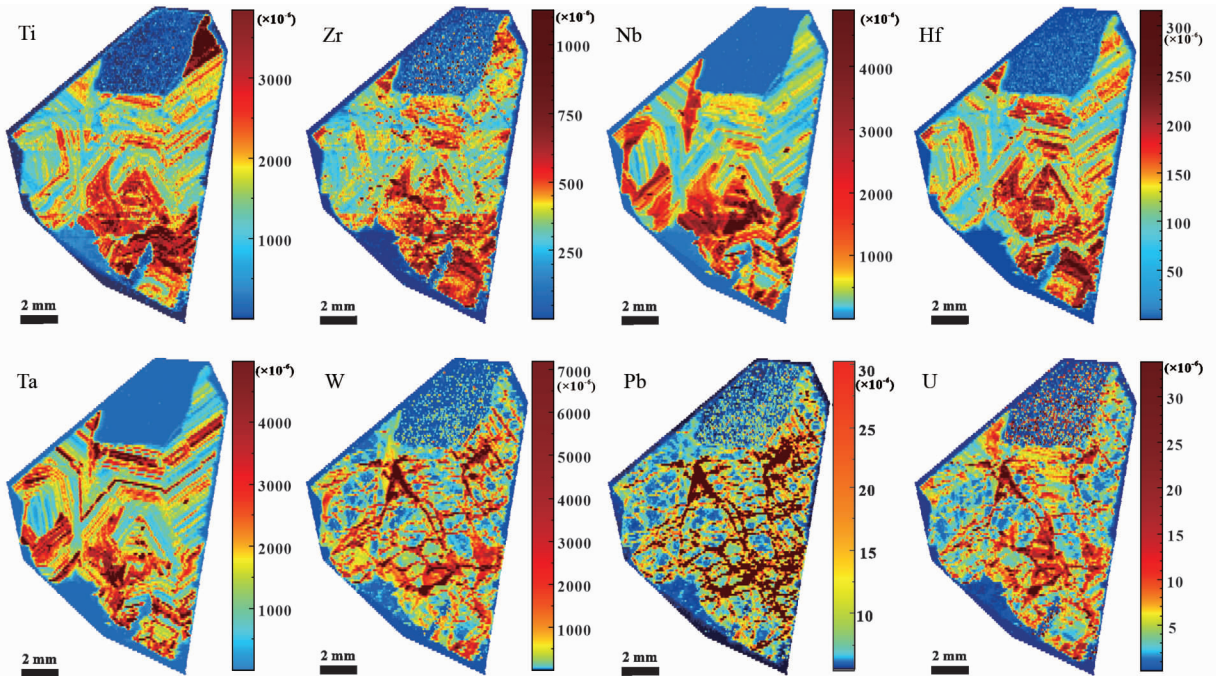


图9 锡石 Kard 激光二维扫描图

Fig. 9 The trace element mapping of Kard cossiterite using LA-ICP-MS

一方面能够快速锁定高 U/Pb 区域,实现高铀区域的精准 U-Pb 定年 (Yang *et al.*, 2020, 2021, 2022a; 杨明等, 2021; 杨岳衡等, 2021; Wei *et al.*, 2022; 吴石头等, 2022; 杨明, 2022)。

针对普通铅校正的问题,由于低 U 矿物的标准物质也往往含普通铅,这对校正方法提出了新的要求,低铀矿物激光微区 U-Pb 分馏校正,目前多采用与方解石激光 U-Pb 分馏校正类似方法来解决 (吴石头等, 2022)。激光 U-Pb 定年的激光剥蚀过程中,不同元素之间分馏较大 (U/Pb, 5% ~ 10%, 不同矿物之间差别较大),同一元素的同位素之间分馏较小 ( $^{207}\text{Pb}/^{206}\text{Pb}$ , 通常小于 1%),因此,  $^{207}\text{Pb}/^{206}\text{Pb}$  多采用标准玻璃 (NIST 或 ARM) 校正,  $^{206}\text{Pb}/^{238}\text{U}$  则采用已知 ID-TIMS 年龄的同种矿物校正,多家实验室也证明该方案的可行性 (Neymark *et al.*, 2018; Tang *et al.*, 2020, 2022; 吴石头等, 2022)。低铀实际样品微区 U-Pb 定年,构建 Tera-Wasserburg 图解,直接获得下交点年龄是普遍采用的方案,适合绝大多数铌钽矿、锡石、黑钨矿和白钨矿,而部分低普通铅锡石,也可以采用  $^{208}\text{Pb}$  校正,构筑谐和 U-Pb 年龄 (Yang *et al.*, 2022a)。因此,无需低普通铅的矿物微区 U-Pb 标准物质,只需其均一的 U-Pb 年龄,就可以进行激光微区 U-Pb 定年的分馏校正。

尽管铌钽矿微区 U-Pb 标准物质有了更多选择,鉴于铌钽矿的主量变化太大,不同端元均一的微区铌钽矿 U-Pb 标准物质仍然缺乏,已知 ID-TIMS 年龄的铌钽矿标准物质,仍然局限在少数实验室 (表 4)。而氟碳铈矿、磷钇矿、黑钨矿、白钨矿微区 U-Pb 标准物质的种类与数量都亟需加强,特别

是白钨矿,目前只有一个白钨矿 ID-TIMS 年龄结果,而实验室内标准迫切需要进行 ID-TIMS U-Pb 标定。尽管有研究表明,如氧逸度条件的变化可能是控制白钨矿 U 含量的主要因素,如白钨矿铀与稀土等其他微量元素之间的关系等方面,相关的工作研究和数据积累有待加强与检验 (Song *et al.*, 2019; Li *et al.*, 2023; Wu *et al.*, 2023)。已有文献的铌钽矿、锡石和黑钨矿的 ID-TIMS U-Pb 年龄绝大多数在德国地质研究中心 Romer 教授实验室完成。国内基本具备这方面的能力,已经有单颗粒锆石 ID-TIMS U-Pb 方法及应用研究报告,亟待加强这方面工作 (Chu *et al.*, 2016; 储著银等, 2016; 王伟等, 2020)。

同时,碰撞反应池技术的出现,可能为强峰拖尾干扰的消除,提供了新的思路,如铌钽矿 Ta 和黑钨矿 W 对激光 Hf 同位素测定的难题。而针对以往 LA-ICP-MS 无法进行  $^{204}\text{Pb}$  校正的难题,由于氦气能够跟汞反应,准确实现  $^{204}\text{Pb}$  测定,有望 LA-ICP-MS/MS 和 SIMS 一样,实验  $^{204}\text{Pb}$  准确扣除 (Gilbert and Glorie, 2020; Xiang *et al.*, 2021)。

稀有金属矿物成矿物质源区示踪方面,铌钽矿、锡石激光微区 Hf 同位素和白钨矿激光微区 Sr-Nd 同位素的应用研究才刚刚开始 (Li *et al.*, 2018; Song *et al.*, 2019; Tang *et al.*, 2021; Yang *et al.*, 2023a),相对高 Hf 含量铌钽矿/锡石、高 Sr/Nd 含量白钨矿样品的地球化学特征也有待更多研究工作与数据积累,才有可能揭示相关的规律,白钨矿微区 Sr-Nd 同位素标准物质研发也需要进一步加强。

## 8.2 激光微区 Rb-Sr/Lu-Hf 定年

虽然目前激光微区 Rb-Sr/Lu-Hf 定年精度还低于传统溶

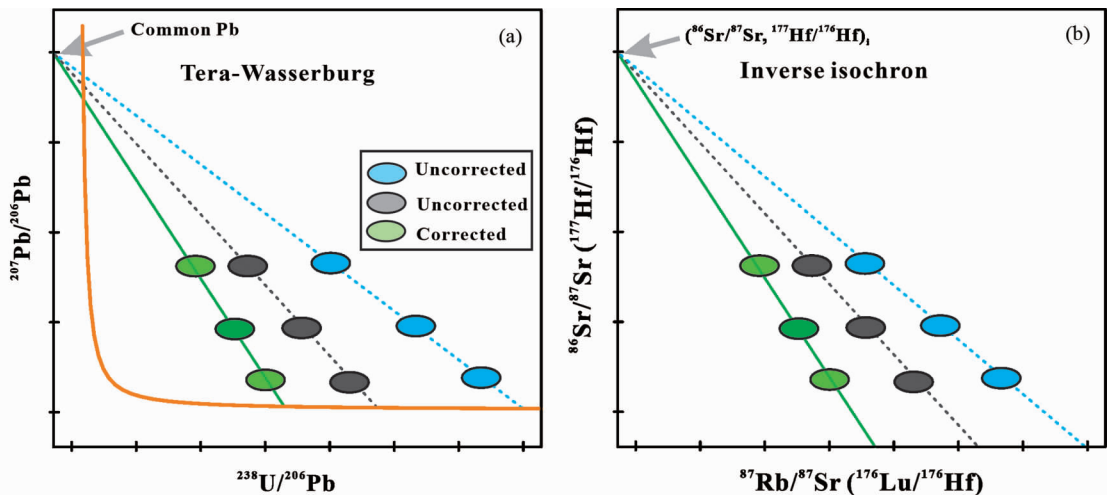


图 10 微区 U-Pb 定年 Tera-Wasserburg 与 Rb-Sr/Lu-Hf 定年反等时线图

Fig. 10 Plot of *in situ* U-Pb age of Tera-Wasserburg and Rb-Sr/Lu-Hf age of inverse age

液法,但存在以下优势:(1)样品制备较简单,可以在探针片上直接进行,这种对目标矿物的原位测定,保留了矿物之间的原始岩相学关系,有利于数据的解读,也避免了耗时的矿物分选、化学分离与质谱测试等诸多繁琐过程(Simpson *et al.*, 2021, 2022);(2)测试速度较快,实时在线获得测试结果,测试成本相对较低,可以快速获得大量数据,为区域的筛查提供快捷工具;(3)空间分辨率的显著提升( $<100\mu\text{m}$ ),可以实现单点测定,能实现单颗粒矿物中的生长环带的精细研究,能揭示更多常规溶液方法不能识别的期次,而且可以将年龄信息与变质结构、温压条件联系起来(Brown *et al.*, 2022; Tamblyn *et al.*, 2022);(4)可以同时获得 U-Pb 和/或 Rb-Sr/Lu-Hf 年龄与同位素信息,不同同位素体系给出的年龄差异与多元同位素信息可以更好地约束样品的形成过程(Gillespie *et al.*, 2022; Glorie *et al.*, 2023)。这些最新发表在国际学术杂志上的工作充分显示了这一技术的优越性,以及在解决相关问题研究的巨大潜力,是未来微区分析地球化学的前沿与热点(王浩等, 2022)。

尽管目前激光微区 Rb-Sr/Lu-Hf 定年获得了很多不同于前人的认识,显示了新兴技术的巨大潜力,但是仍处于起步阶段,相关的方法技术尚不成熟,有三方面问题迫切需要解决:

(1)实验方法 首先是反应气离子反应产率的量化与稳定性需要评估。理论上,只有 Sr/Hf 发生离子反应,而 Rb/Yb/Lu 则不反应,实际情况可能并非如此,或者需要量化。其次,初始同位素比值对定年结果的影响需要评估,如 Rb/Sr 或 Lu/Hf 比,对模式年龄与等时线年龄的影响,如何准确获得母体比( $^{87}\text{Rb}/^{86}\text{Sr}$ 、 $^{176}\text{Lu}/^{177}\text{Hf}$ )和放射性子体比( $^{87}\text{Sr}/^{86}\text{Sr}$ 、 $^{176}\text{Hf}/^{177}\text{Hf}$ )等。与激光 U-Pb 定年类似,在激光剥蚀过程中,母体之间分馏较大,而同种矿物组成的标准物质来校正其分馏是最理想方案。在数据结果表述上,激光微区 Rb-Sr/Lu-Hf 定年,与 U-Pb 定年类似,有等时线和反等时线

两种方式(图 10),尤其是反等时线法,更加适合同位素比值线性变化的年龄均一的标准物质,通过初始同位素( $^{207}\text{Pb}/^{206}\text{Pb}$ 、 $^{86}\text{Sr}/^{87}\text{Sr}$ 、 $^{177}\text{Hf}/^{176}\text{Hf}$ )固定上交点,其下交点( $^{238}\text{U}/^{206}\text{Pb}$ 、 $^{87}\text{Rb}/^{87}\text{Sr}$ 、 $^{176}\text{Lu}/^{176}\text{Hf}$ )就可以计算获得样品的年龄(Popov, 2022; Simpson *et al.*, 2022)。

(2)标准物质 激光用户的快速增长以及激光的有损分析,大大增加了标准物质的消耗与需求。同时,不同年龄范围的多种标准物质,有助于数据质量的监控和保障。但无论从矿物种类还是数量而言,同种矿物组成标准物质的严重缺乏,是当前激光微区 Rb-Sr/Lu-Hf 定年实际应用受限的主要障碍与瓶颈。对于激光原位 Rb-Sr 定年而言,只有粉末压片的黑云母和金云母标准物质(Mica-Mg 和 Mica-Fe)在使用;但是,粉末压片与天然矿物的剥蚀特征和分馏模式相比仍存在差异,采用与目标矿物基体匹配的标准物质,对进一步提高年龄的准确性至关重要(Redaa *et al.*, 2021, 2023)。而锂云母、铁锂云母、天河石、铯沸石等稀有金属矿物还没有相应的标准物质,与已有的黑云母和金云母是否存在基体效应,还需要系统的评估。对于激光微区 Lu-Hf 定年而言,除了磷钇矿、磷灰石可以使用已有 U-Pb 标准物质外,石榴石、方解石、萤石等没有相应标准物质,而其他潜在的激光微区 Lu-Hf 定年矿物(硅铍钇矿、易解石、黑稀金矿、独居石、褐帘石、黑钨矿、白钨矿等)还未见报道。

(3)激光质谱 由于市场占有率的原因,当前绝大多数工作都是基于 8800/8900 ICP-MS/MS 开展,其他类型仪器(如热电公司 i CAP TQ ICP-MS/MS 和珀金埃尔默公司 NexION 5000 ICP-MS/MS)还极少有报道。纳秒与飞秒激光的剥蚀行为,对 Rb-Sr/Lu-Hf 定年的影响,及其基体效应也亟需研究。无论从仪器灵敏度还是同位素比值精度看,多接收磁式等离子质谱都要优于四级杆等离子质谱,带碰撞反应池多接收等离子质谱(热电公司 Neoma MC-ICP-MS/MS),其激光原位 Rb-Sr 或 Lu-Hf 定年结果都会优于四级杆等离子质谱,有望



实现高空间分辨率或高精度的年轻样品微区 Rb-Sr 或 Lu-Hf 精细年代学研究,当然四级杆等离子质谱的优势则是经济、便捷,适合快速的大面积扫描工作研究。此外,激光原位 Rb-Sr 或 Lu-Hf 定年研究,对其他  $\beta$  衰变体系的激光微区 Re-Os/K-Ca 定年也有很好的启示与借鉴意义。

## 9 结语

以上我们对目前常见稀有金属矿物的 U-Pb 定年体系和可能的 Sr-Nd-Hf 同位素示踪应用进行了总结。需要指出的是,这些方法和技术并非现在独有。传统的云母 Rb-Sr、石榴石 Sm-Nd 和锆石 U-Pb 定年等都能对稀有金属矿床的成因与演化提供重要约束。但对稀有金属矿物直接进行同位素测年和同位素示踪,无疑是了解矿床形成时代和成矿物质来源的最直接手段。此外,近年来金属稳定同位素领域发展迅速,并在稀有金属矿床成因研究中得到广泛应用(韦刚健等, 2022)。就上述稀有金属矿物而言,Fe、Mg、Ca、Zn、Ba、Mo、Zr、Sn、Si、B、Li、K、Rb 等同位素体系的开发与应用,都是未来值得重视的研究领域。

由于稀有金属成矿过程的复杂性,矿物分选并不是微区测试分析的最佳方式,薄片直接测试是最理想的,因此测试前详实的岩相学工作必不可少,也有利于后期数据的解读。实验方法研发、标准物质研发是相辅相成、相互促进的,也是当前迫切需要解决的关键技术难题。只有这样,激光微区 U-Pb/Rb-Sr/Sm-Nd/Lu-Hf 定年和 Sr/Nd/Hf 同位素示踪才会像成熟的锆石 U-Pb 定年与 Hf 同位素一样成为一种常规的手段而广泛应用。总而言之,随着黑钨矿、白钨矿、锡石、铌钽矿、氟碳铈矿、磷钇矿、锂云母、铁锂云母、铯沸石、钾长石(天河石)等稀有金属矿物激光微区 U-Pb/Rb-Sr/Lu-Hf 年代学方法的不断成熟和日趋完善,相关技术难题正在或即将得到解决,显示该方法广泛的应用与推广前景。战略性稀有金属已经成为国内外成矿作用研究新的热点与前沿,钨锡铌钽铍铀铯稀土等稀有金属矿物微区成矿年代学方法,必将为我国新一轮矿床学研究做出应有的学术贡献。

**致谢** 由于涉及的研究资料和文献实在太多,作者难以一一注明,敬请原作者和读者见谅。两位匿名审稿人和编辑老师的意见进一步完善了论文,一并致以诚挚谢意。

## References

Aldrich LT, Davis GL, Tilton GR and Wetherill GW. 1956. Radioactive ages of minerals from the Brown Derby Mine and the Quartz Creek Granite near Gunnison, Colorado. *Journal of Geophysical Research*, 61(2): 215–232

Altenberger U, Rojas-Agramonte Y, Yang YH, Fernández-Lamus J, Häger T, Guenter C, Gonzalez-Pinzón A, Charris-Leal F and Artel J. 2022. *In situ* U-Th-Pb dating of parisite: Implication for the age of Mineralization of Colombian Emeralds. *Minerals*, 12(10): 1232

Bevan D, Coath CD, Lewis J, Schwieters J, Lloyd N, Craig G, Wehrs H and Elliott T. 2021. *In situ* Rb-Sr dating by collision cell, multicollection inductively-coupled plasma mass-spectrometry with pre-cell mass-filter, (CC-MC-ICPMS/MS). *Journal of Analytical Atomic Spectrometry*, 36(5): 917–931

Bolea-Fernandez E, Van Malderen SJM, Balcaen L, Resano M and Vanhaecke F. 2016a. Laser ablation-tandem ICP-mass spectrometry (LA-ICP-MS/MS) for direct Sr isotopic analysis of solid samples with high Rb/Sr ratios. *Journal of Analytical Atomic Spectrometry*, 31(2): 464–472

Bolea-Fernandez E, Balcaen L, Resano M and Vanhaecke F. 2016b. Tandem ICP-mass spectrometry for Sr isotopic analysis without prior Rb/Sr separation. *Journal of Analytical Atomic Spectrometry*, 31(1): 303–310

Bolea-Fernandez E, Balcaen L, Resano M and Vanhaecke F. 2017. Overcoming spectral overlap via inductively coupled plasma-tandem mass spectrometry (ICP-MS/MS): A tutorial review. *Journal of Analytical Atomic Spectrometry*, 32(9): 1660–1679

Bolea-Fernandez E, Rua-Ibarz A, Resano M and Vanhaecke F. 2021. To shift, or not to shift: Adequate selection of an internal standard in mass-shift approaches using tandem ICP-mass spectrometry (ICP-MS/MS). *Journal of Analytical Atomic Spectrometry*, 36(6): 1135–1149

Brown DA, Simpson A, Hand M, Morrissey LJ, Gilbert S, Tamblyn R and Glorie S. 2022. Laser-ablation Lu-Hf dating reveals Laurentian garnet in subducted rocks from southern Australia. *Geology*, 50(7): 837–842

Cao JY, Yang XY, Zhang DX and Yan FB. 2020. *In situ* trace elements and Sr isotopes in scheelite and S-Pb isotopes in sulfides from the Shiweidong W-Cu deposit, giant Dahutang ore field: Implications to the fluid evolution and ore genesis. *Ore Geology Reviews*, 125: 103696

Carr PA, Norman MD and Bennett VC. 2017. Assessment of crystallographic orientation effects on secondary ion mass spectrometry (SIMS) analysis of cassiterite. *Chemical Geology*, 467: 122–133

Carr PA, Zink S, Bennett VC, Norman MD, Amelin Y and Blevin PL. 2020. A new method for U-Pb geochronology of cassiterite by ID-TIMS applied to the Mole Granite polymetallic system, eastern Australia. *Chemical Geology*, 539: 119539

Carr PA, Moreira E, Neymark L, Norman MD and Mercadier J. 2023. A LA-ICP-MS comparison of reference materials used in cassiterite U-Pb geochronology. *Geostandards and Geoanalytical Research*, 47(1): 67–87

Che XD, Wu FY, Wang RC, Gerdes A, Ji WQ, Zhao ZH, Yang JH and Zhu ZY. 2015. *In situ* U-Pb isotopic dating of columbite-tantalite by LA-ICP-MS. *Ore Geology Reviews*, 65: 979–989

Che XD, Wang RC, Wu FY, Zhu ZY, Zhang WL, Hu H, Xie L, Lu JJ and Zhang D. 2019. Episodic Nb-Ta mineralisation in South China: Constraints from *in situ* LA-ICP-MS columbite-tantalite U-Pb dating. *Ore Geology Reviews*, 105: 71–85

Chen J, Hou KJ, Wang Q, Yuan SD and Chen YL. 2021. *In situ* U-Pb dating of cassiterite by LA-ICP-MS without a matrix-matched standard. *Acta Petrologica Sinica*, 37(3): 943–955 (in Chinese with English abstract)

Chu ZY, He HY, Ramezani J, Bowring SA, Hu DY, Zhang LJ, Zheng SL, Wang XL, Zhou ZH, Deng CL and Guo JH. 2016. High-precision U-Pb geochronology of the Jurassic Yanliao Biota from Jianchang (western Liaoning Province, China): Age constraints on the rise of feathered dinosaurs and eutherian mammals. *Geochemistry, Geophysics, Geosystems*, 17(10): 3983–3992

Chu ZY, Xu JJ, Chen Z, Li CF, Li XH, He HY, Li XH and Guo JH. 2016. Ultra-low blank analytical procedure for high precision CA-ID-TIMS U-Pb dating of single grain zircons. *Chinese Science Bulletin*, 61(10): 1121–1129 (in Chinese with English abstract)

Craig G, Wehrs H, Bevan DG, Pfeifer M, Lewis J, Coath CD, Elliott T, Huang C, Lloyd NS and Schwieters JB. 2021. Project vienna: A novel pre-cell mass filter for collision/reaction cell MC-ICPMS/MS.

- Analytical Chemistry, 93(30): 10519–10527
- Cruz-Urbe AM, Craig G, Garber JM, Paul B, Arkula C and Bouman C. 2023. Single spot Rb-Sr isochron dating of biotite by LA-MC-ICP-MS/MS. *Geostandards and Geoanalytical Research*, 47(4): 795–809
- Cui YR, Tu JR, Chen F, Hao S, Ye LJ, Zhou HY and Li HM. 2017. The research advances in LA-(MC)-ICP-MS U-Pb dating of cassiterite. *Acta Geologica Sinica*, 91(6): 1386–1399 (in Chinese with English abstract)
- Dauphas N, Hopp T, Craig G, Zhang ZJ, Valdes MC, Heck PR, Charlier BLA, Bell EA, Harrison TM, Davis AM, Dussubieux L, Williams PR, Krawczynski MJ, Bouman C, Lloyd NS, Tollstrup D and Schwieters JB. 2022. *In situ*  $^{87}\text{Rb}$ - $^{87}\text{Sr}$  analyses of terrestrial and extraterrestrial samples by LA-MC-ICP-MS/MS with double Wien filter and collision cell technologies. *Journal of Analytical Atomic Spectrometry*, 37(11): 2420–2441
- Deng XD, Li JW, Zhao XF, Hu ZC, Hu H, Selby D and de Souza ZS. 2013. U-Pb isotope and trace element analysis of columbite-(Mn) and zircon by laser ablation ICP-MS; Implications for geochronology of pegmatite and associated ore deposits. *Chemical Geology*, 344: 1–11
- Deng XD, Luo T, Li JW and Hu ZC. 2019. Direct dating of hydrothermal tungsten mineralization using *in situ* wolframite U-Pb chronology by laser ablation ICP-MS. *Chemical Geology*, 515: 94–104
- Deng XH, Chen YJ, Bagas L, Li HM, Zhou HY, Yuan SD and Li DF. 2018a. Reply to and comment on “the usage of  $^{238}\text{U}/^{207}\text{Pb}$  vs  $^{206}\text{Pb}/^{207}\text{Pb}$  linear regressions for the LA-ICP-MS U-Pb dating of cassiterite”. *Ore Geology Reviews*, 95: 1188–1190
- Deng XH, Chen YJ, Bagas L, Zhou HY, Zheng Z, Yue SW, Chen HJ, Li HM, Tu JR and Cui YR. 2018b. Cassiterite U-Pb geochronology of the Kekakaerde W-Sn deposit in the Baiganhu ore field, East Kunlun Orogen, NW China: Timing and tectonic setting of mineralization. *Ore Geology Reviews*, 100: 534–544
- Denholm JL, Stepanov AS, Meffre S, Bottrill RS and Thompson JM. 2021. The geochronology of Tasmanian tin deposit using LA-ICP-MS U-Pb cassiterite dating. *Economic Geology*, 116: 1387–1407
- Dewaele S, Henjes-Kunst F, Melcher F, Sitnikova M, Burgess R, Gerdes A, Fernandez MA, De Clercq F, Muchez P and Lehmann B. 2011. Late Neoproterozoic overprinting of the cassiterite and columbite-tantalite bearing pegmatites of the Gatumba area, Rwanda (Central Africa). *Journal of African Earth Sciences*, 61(1): 10–26
- Dill HG, Gerdes A and Weber B. 2007. Cu-Fe-U phosphate mineralization of the Hagendorf-Pleystein pegmatite province, Germany: With special reference to laser-ablation inductively-coupled plasma mass spectrometry (LA-ICP-MS) of limonite-cored torbernite. *Mineralogical Magazine*, 71(4): 371–387
- Fletcher IR, Rasmussen B and McNaughton NJ. 2000. SHRIMP U-Pb geochronology of authigenic xenotime and its potential for dating sedimentary basins. *Australian Journal of Earth Sciences*, 47(5): 845–859
- Fletcher IR, McNaughton NJ, Aleinikoff JA, Rasmussen B and Kamo SL. 2004. Improved calibration procedures and new standards for U-Pb and Th-Pb dating of Phanerozoic xenotime by ion microprobe. *Chemical Geology*, 209(3–4): 295–314
- Foster GL and Vance D. 2006. *In situ* Nd isotopic analysis of geological materials by laser ablation MC-ICP-MS. *Journal of Analytical Atomic Spectrometry*, 21(3): 288–296
- Frei R, Nägler TF, Schönberg R and Kramers JD. 1998. Re-Os, Sm-Nd, U-Pb and stepwise lead leaching isotope systematics in shear-zone hosted gold mineralization: Genetic tracing and age constraints of crustal hydrothermal activity. *Geochimica et Cosmochimica Acta*, 62(11): 1925–1936
- Gäbler HE, Melcher F, Graupner T, Bahr A, Sitnikova MA, Henjes-Kunst F, Oberthür T, Brätz H and Gerdes A. 2011. Speeding up the analytical workflow for coltan fingerprinting by an integrated mineral liberation analysis/LA-ICP-MS approach. *Geostandards and Geoanalytical Research*, 35(4): 431–448
- Gilbert SE and Glorie S. 2020. Removal of Hg interferences for common Pb correction when dating apatite and titanite by LA-ICP-MS/MS. *Journal of Analytical Atomic Spectrometry*, 35(7): 1472–1481
- Gillespie J, Kirkland CL, Kinny PD, Simpson A, Glorie S and Rankenburg K. 2022. Lu-Hf, Sm-Nd and U-Pb isotopic coupling and decoupling in apatite. *Geochimica et Cosmochimica Acta*, 338: 121–135
- Glorie S, Burke T, Hand M, Simpson A, Gilbert S and Wade B. 2022. *In situ* Lu-Hf phosphate geochronology: Progress towards a new tool for space exploration. *Geoscience Frontiers*, 13(3): 101375
- Glorie S, Hand M, Mulder J, Simpson A, Emo RB, Kamber B, Fernie N, Nixon A and Glibert S. 2023. Robust laser ablation Lu-Hf dating of apatite: An empirical evaluation. Geological Society, London, Special Publications, 537: 165–184
- Goodey MA, Tapster SR, Roberts NMW, Gardiner NJ, Robb LJ, Shail RK and Bista D. 2023. Turning advances in high-precision cassiterite U-Pb geochronology into improved mineral system models. *Goldschmidt*, 164
- Gorojovsky L and Alard O. 2020. Optimisation of laser and mass spectrometer parameters for the *in situ* analysis of Rb/Sr ratios by LA-ICP-MS/MS. *Journal of Analytical Atomic Spectrometry*, 35(10): 2322–2336
- Gou LL, Long XP, Yan HY, Shu TC, Wang JY, Xu XF, Zhou F and Tian ZB. 2022. Metamorphic *P-T* evolution and *in situ* biotite Rb-Sr geochronology of garnet-staurolite schist from the Ramba gneiss dome in the Northern Himalaya. *Frontiers in Earth Science*, 10: 887154
- Gulson BL and Jones MT. 1992. Cassiterite: Potential for direct dating of mineral deposits and a precise age for the Bushveld Complex granites. *Geology*, 20(4): 355–358
- Gyomlai T, Agard P, Jolivet L, Larvet T, Bonnet G, Omrani J, Larson K, Caron B and Noël J. 2022. Cimmerian metamorphism and post Mid-Cimmerian exhumation in Central Iran: Insights from *in-situ* Rb/Sr and U/Pb dating. *Journal of Asian Earth Sciences*, 233: 105242
- Han JS, Chen HY, Hong W, Hollings P, Chu GB, Zhang L and Sun SQ. 2020. Texture and geochemistry of multi-stage hydrothermal scheelite in the Tongshankou porphyry-skarn Cu-Mo(-W) deposit, eastern China: Implications for ore-forming process and fluid metasomatism. *American Mineralogist*, 105(6): 945–954
- Hao S, Li HM, Li GZ, Geng JZ, Zhou HY, Xiao ZB, Cui YR and Tu JR. 2016. The comparison of the principle and applicability between two methods of deducting the initial common lead for *in situ* LA-ICP-MS U-Pb isotope dating of cassiterite. *Geological Bulletin of China*, 35(4): 622–632 (in Chinese with English abstract)
- Harlaux M, Romer RL, Mercadier J, Morlot C, Marignac C and Cuney M. 2018a. 40Ma of hydrothermal W mineralization during the Variscan orogenic evolution of the French Massif Central revealed by U-Pb dating of wolframite. *Mineralium Deposita*, 53(1): 21–51
- Harlaux M, Mercadier J, Marignac C, Peiffert C, Cloquet C and Cuney M. 2018b. Tracing metal sources in peribatholithic hydrothermal W deposits based on the chemical composition of wolframite: The example of the Variscan French Massif Central. *Chemical Geology*, 479: 58–85
- Hogmalm KJ, Zack T, Karlsson AKO, Sjöqvist ASL and Garbe-Schönberg D. 2017. *In situ* Rb-Sr and K-Ca dating by LA-ICP-MS/MS: An evaluation of  $\text{N}_2\text{O}$  and  $\text{SF}_6$  as reaction gases. *Journal of Analytical Atomic Spectrometry*, 32(2): 305–313
- Hou KJ, Qin Y, Li YH and Fan CF. 2013. *In situ* Sr-Nd isotopic measurement of apatite using laser ablation multi-collector inductively coupled plasma-mass spectrometry. *Rock and Mineral Analysis*, 32(4): 547–554 (in Chinese with English abstract)
- Huang C, Wang H, Shi WB, Sun JF, Hu FY, Xu L, Yang YH, Wu ST, Xie LW and Yang JH. 2023. *In situ* Rb-Sr dating of mica by LA-ICP-MS/MS. *Science China (Earth Sciences)*, 66(11): 2603–2621
- Huang SQ, Chang ZS, Liu KR and Garbe-Schönberg D. 2023. Optimisation of LA-ICP-MS/MS Rb-Sr dating of micas with non-

- matrix-matched reference materials. *Geostandards and Geoanalytical Research*, 47(4): 725–747
- Iizuka T, Eggins SM, McCulloch MT, Kinsley LPJ and Mortimer GE. 2011. Precise and accurate determination of  $^{147}\text{Sm}/^{144}\text{Nd}$  and  $^{143}\text{Nd}/^{144}\text{Nd}$  in monazite using laser ablation-MC-ICPMS. *Chemical Geology*, 282(1–2): 45–57
- Jegal Y, Zimmermann C, Reisberg L, Yeghicheyan D, Cloquet C, Peiffert C, Gerardin M, Deloule E and Mercadier J. 2022. Characterisation of reference materials for *in situ* Rb-Sr dating by LA-ICP-MS/MS. *Geostandards and Geoanalytical Research*, 46(4): 645–671
- Jiang SY, Zhao KD, Jiang H, Su HM, Xiong SF, Xiong YQ, Xu YM, Zhang W and Zhu LY. 2020. Spatiotemporal distribution, geological characteristics and metallogenic mechanism of tungsten and tin deposits in China: An overview. *Chinese Science Bulletin*, 65(33): 3730–3745 (in Chinese with English abstract)
- Jiang SY, Wang CL, Zhang L, Yuan F, Su HM, Zhang HX and Liu T. 2021. *In situ* trace element tracing and isotopic dating of pegmatite type lithium deposits: An overview. *Acta Geologica Sinica*, 95(10): 3017–3038 (in Chinese with English abstract)
- Kelepile T, Betsi TB and Shemang E. 2023. The Late Neoproterozoic sediment-hosted Kalahari Copper Belt in Botswana: Refining the genetic model with sericite Ar/Ar and *in situ* LA-ICP-MS biotite Rb/Sr geochronology. *International Geology Review*, 65(22): 3523–3543
- Kendall-Langley LA, Kemp AIS, Grigson JL and Hammerli J. 2020. U-Pb and reconnaissance Lu-Hf isotope analysis of cassiterite and columbite group minerals from Archean Li-Cs-Ta type pegmatites of Western Australia. *Lithos*, 352–353: 105231
- Kharkongor MBK, Glorie S, Mulder J, Kirkland CL, Chew D, Kohn B and Simpson A. 2023. Apatite laser ablation Lu-Hf geochronology: A new tool to date mafic rocks. *Chemical Geology*, 636: 121630
- Kozlik M, Gerdes A and Raith JG. 2016. Strontium isotope systematics of scheelite and apatite from the Felbertal tungsten deposit, Austria—results of *in situ* LA-MC-ICP-MS analysis. *Mineralogy and Petrology*, 110(1): 11–27
- Lana C, Gonçalves GO, Mazoz A, Buick I, Kamo S, Scholz R, Wang H, Moreira H, Babinski M and Queiroga G. 2022. Assessing the U-Pb, Sm-Nd and Sr-Sr isotopic compositions of the Sumé apatite as a reference material for LA-ICP-MS analysis. *Geostandards and Geoanalytical Research*, 46(1): 71–95
- Larson KP, Button M, Shrestha S and Camacho A. 2023. A comparison of  $^{87}\text{Rb}/^{87}\text{Sr}$  and  $^{40}\text{Ar}/^{39}\text{Ar}$  dates: Evaluating the problem of excess  $^{40}\text{Ar}$  in Himalayan mica. *Earth and Planetary Science Letters*, 609: 118058
- Laureijs CT, Congan LA and Spence J. 2021. *In situ* Rb-Sr dating of celadonite from altered upper oceanic crust using laser ablation ICP-MS/MS. *Chemical Geology*, 579: 120339
- Lecumberri-Sanchez P, Romer RL, Lüders V and Bodnar RJ. 2014. Genetic relationship between silver-lead-zinc mineralization in the Wutong deposit, Guangxi Province and Mesozoic granitic magmatism in the Nanling belt, Southeast China. *Mineralium Deposita*, 49(3): 353–369
- Legros H, Mercadier J, Villeneuve J, Romer RL, Deloule E, van Lichtervelde M, Dewaele S, Lach P, Che XD, Wang RC, Zhu ZY, Gloaguen E and Melleton J. 2019. U-Pb isotopic dating of columbite-tantalite minerals: Development of reference materials and *in situ* applications by ion microprobe. *Chemical Geology*, 512: 69–84
- Legros H, Harlaux M, Mercadier J, Romer RL, Poujol M, Camacho A, Marignac C, Cuney M, Wang RC, Charles N and Lespinasse MY. 2020. The world-class Nanling metallogenic belt (Jiangxi, China): W and Sn deposition at 160Ma followed by 30m. y. of hydrothermal metal redistribution. *Ore Geology Reviews*, 117: 103302
- Li C, Zhou LM, Zhao Z, Zhang ZY, Zhao H, Li XW and Qu WJ. 2018. *In situ* Sr isotopic measurement of scheelite using fs-LA-MC-ICPMS. *Journal of Asian Earth Sciences*, 160: 38–47
- Li CY, Zhang RQ, Ding X, Ling MX, Fan WM and Sun WD. 2016. Dating cassiterite using laser ablation ICP-MS. *Ore Geology Reviews*, 72: 313–322
- Li JK, Li P, Yan QG, Wang DH, Ren GL and Ding X. 2023. Geology and mineralization of the Songpan-Ganze-West Kunlun pegmatite-type rare-metal metallogenic belt in China: An overview and synthesis. *Science China (Earth Sciences)*, 66(8): 1702–1724
- Li QL, Li XH, Lan ZW, Guo CL, Yang YN, Liu Y and Tang GQ. 2013. Monazite and xenotime U-Th-Pb geochronology by ion microprobe: Dating highly fractionated granites at Xihuashan tungsten mine, SE China. *Contributions to Mineralogy and Petrology*, 166(1): 65–80
- Li QL, Huyskens MH, Yang YH, Ling XX, Yin QZ, Nikiforov AV and Li XH. 2020a. Bastnaesite K-9: A homogenous natural reference material for *in situ* U-Pb and Th-Pb dating. *Atomic Spectroscopy*, 41(6): 218–222
- Li SS, Santosh M, Farkaš J, Redaa A, Ganguly S, Kim SW, Zhang C, Gilbert S and Zack T. 2020b. Coupled U-Pb and Rb-Sr laser ablation geochronology trace Archean to Proterozoic crustal evolution in the Dharwar Craton, India. *Precambrian Research*, 343: 105709
- Li W, Xie GQ, Cook NJ, Mao JW, Li C, Ciobanu CL and Zhang ZY. 2021. Tracking dynamic hydrothermal processes: Textures, *in situ* Sr-Nd isotopes and trace-element analysis of scheelite from the Yangjiashan vein-type W deposit, South China. *American Mineralogist*, 106(12): 1987–2002
- Li Y, Yang YH, Jiao SJ, Wu FY, Yang JH, Xie LW and Huang C. 2015. *In situ* determination of hafnium isotopes from rutile using LA-MC-ICP-MS. *Science China Earth Sciences*, 58(12): 2134–2144
- Li Y, Yuan F, Jowitt SM, Li XL, Zhou TF, Wang FY and Deng YF. 2023. Combined garnet, scheelite and apatite U-Pb dating of mineralizing events in the Qiaomaishan Cu-W skarn deposit, eastern China. *Geoscience Frontiers*, 14(1): 101459
- Liebmann J, Kirkland CL, Kelsey DE, Korhonen FJ and Rankenburg K. 2022. Lithological fabric as a proxy for Rb-Sr isotopic complexity. *Chemical Geology*, 608: 121041
- Lihter I, Larson KP, Smit MA, Cottle JM, Ashley KT and Shrestha S. 2022. Decrypting the polymetamorphic record of the Himalaya. *Geology*, 50(5): 588–592
- Ling XX, Li QL, Liu Y, Yang YH, Liu Y, Tang GQ and Li XH. 2016. *In situ* SIMS Th-Pb dating of bastnaesite: Constraint on the mineralization time of the Himalayan Mianning-Dechang rare earth element deposits. *Journal of Analytical Atomic Spectrometry*, 31(8): 1680–1687
- Ling XX, Huyskens MH, Li QL, Yin QZ, Werner R, Liu Y, Tang GQ, Yang YN and Li XH. 2017. Monazite RW-1: A homogenous natural reference material for SIMS U-Pb and Th-Pb isotopic analysis. *Mineralogy and Petrology*, 111(2): 163–172
- Liu RP, Guo DF, Xie SK and Li L. 2022. A potential working reference material for *in situ* U-Pb dating of cassiterite. The 11<sup>th</sup> International Conference on the Analysis of Geological and Environmental Materials, A84
- Liu YP, Li ZX, Li HM, Guo LG, Xu W, Ye L, Li CY and Pi DH. 2007. U-Pb geochronology of cassiterite and zircon from the Dulong Sn-Zn deposit: Evidence for Cretaceous large-scale granitic magmatism and mineralization events in southeastern Yunnan Province, China. *Acta Petrologica Sinica*, 23(5): 967–976 (in Chinese with English abstract)
- Liu ZC, Wu FY, Guo CL, Zhao ZF, Yang JH and Sun JF. 2011. *In situ* U-Pb dating of xenotime by laser ablation (LA)-ICP-MS. *Chinese Science Bulletin*, 56(27): 2948–2956
- Liu ZC, Wu FY, Yang YH, Yang JH and Wilde SA. 2012. Neodymium isotopic compositions of the standard monazites used in U-Th-Pb geochronology. *Chemical Geology*, 334: 221–239
- Luo T, Hu ZC, Zhang W, Liu YS, Zong KQ, Zhou L, Zhang JF and Hu SH. 2018. Water vapor-assisted “universal” nonmatrix-matched analytical method for the *in situ* U-Pb dating of zircon, monazite, titanite and xenotime by Laser Ablation-Inductively Coupled Plasma Mass Spectrometry. *Analytical Chemistry*, 90(15): 9016–9024
- Luo T, Deng XD, Li JW, Hu ZC, Zhang W, Liu YS and Zhang JF.

2019. U-Pb geochronology of wolframite by laser ablation inductively coupled plasma mass spectrometry. *Journal of Analytical Atomic Spectrometry*, 34(7): 1439–1446
- Luo T, Zhao H, Zhang W, Guo JL, Zong KQ, Liu YS, Zhang JF and Hu ZC. 2021. Non-matrix-matched analysis of U-Th-Pb geochronology of bastnäsite by laser ablation inductively coupled plasma mass spectrometry. *Science China (Earth Sciences)*, 64(4): 667–676
- Luo T and Hu ZC. 2022. Recent advances in U-Th-Pb dating of accessory minerals by laser ablation inductively coupled plasma mass spectrometry. *Earth Science*, 47(11): 4122–4144 (in Chinese with English abstract)
- Ma Q Evans NJ, Ling XX, Yang JH, Wu FY, Zhao ZD and Yang YH. 2019. Natural titanite reference materials for *in situ* U-Pb and Sm-Nd isotopic measurements by LA-(MC)-ICP-MS. *Geostandards and Geoanalytical Research*, 43(3): 355–384
- Mao JW, Wu SH, Song SW, Dai P, Xie GQ, Su QW, Liu P, Wang XG, Yu ZZ, Chen XY and Tang WX. 2020. The world-class Jiangnan tungsten belt: Geological characteristics, metallogeny and ore deposit model. *Chinese Science Bulletin*, 65(33): 3746–3762 (in Chinese)
- Marini OJ and Botelho NF. 1986. A provincia de granitos estan ferros de Goi s. *Revista Brasileira de Geoci ncias*, 16: 119–131
- McNaughton NJ, Pollard PJ, Gulson BL and Jones MT. 1993. Cassiterite: Potential for direct dating of mineral deposits and a precise age for the Bushveld Complex granites; Comment and Reply. *Geology*, 21(3): 285–286
- Melcher F, Sitnikova MA, Graupner T, Martin N, Oberthür T, Henjes-Kunst F, Gabler E, Gerdes A, Bratz H, Davis DW and Dewaele S. 2008. Fingerprinting of conflict minerals: Columbite-tantalite ('coltan') ores. *SGA News*, (23): 1–14
- Melcher F, Graupner T, Gäbler HE, Sitnikova M, Henjes-Kunst F, Oberthür T, Gerdes A and Dewaele S. 2015. Tantalum-(niobium-tin) mineralisation in African pegmatites and rare metal granites: Constraints from Ta-Nb oxide mineralogy, geochemistry and U-Pb geochronology. *Ore Geology Reviews*, 64: 667–719
- Melcher F, Graupner T, Gäbler HE, Sitnikova M, Oberthür T, Gerdes A, Badanina E and Chudy T. 2017. Mineralogical and chemical evolution of tantalum-(niobium-tin) mineralisation in pegmatites and granites. Part 2: Worldwide examples (excluding Africa) and an overview of global metallogenetic patterns. *Ore Geology Reviews*, 89: 946–987
- Melleton J, Gloaguen E, Frei D, Novák M and Breiter K. 2012. How are the emplacement of rare-element pegmatites, regional metamorphism and magmatism interrelated in the Moldanubian domain of the Variscan Bohemian Massif, Czech Republic? *The Canadian Mineralogist*, 50(6): 1751–1773
- Moens LJ, Vanhaecke FF, Bandura DR, Baranov VI and Tanner SD. 2001. Elimination of isobaric interferences in ICP-MS, using ion-molecule reaction chemistry: Rb/Sr age determination of magmatic rocks, a case study. *Journal of Analytical Atomic Spectrometry*, 16(9): 991–994
- Moscatti RJ and Neymark LA. 2020. U-Pb geochronology of tin deposits associated with the Cornubian Batholith of Southwest England; Direct dating of cassiterite by *in situ* LA-ICPMS. *Mineralium Deposita*, 55(1): 1–20
- Nakai S, Masuda A and Lehmann E. 1988. La-Ba dating of bastnaesite. *American Mineralogist*, 73(9–10): 1111–1113
- Nakai S, Masuda A, Shimizu H and Lu Q. 1989. La-Ba dating and Nd and Sr isotope studies on the Baiyun Obo rare earth element ore deposits, Inner Mongolia, China. *Economic Geology*, 84(8): 2296–2299
- Nazari-Dehkordi T, Spandler C, Oliver NHS and Wilson R. 2018. Unconformity-related rare earth element deposits; A regional-scale hydrothermal mineralization type of northern Australia. *Economic Geology*, 113(6): 1297–1305
- Neymark LA. 2018. Comment on the usage of  $^{238}\text{U}/^{207}\text{Pb}$  vs  $^{206}\text{Pb}/^{207}\text{Pb}$  linear regressions for the LA-ICPMS U-Pb dating of cassiterite. *Ore Geology Reviews*, 95: 1185–1187
- Neymark LA, Holm-Denoma CS and Moscatti RJ. 2018. *In situ* LA-ICPMS U-Pb dating of cassiterite without a known-age matrix-matched reference material; Examples from worldwide tin deposits spanning the Proterozoic to the Tertiary. *Chemical Geology*, 483: 410–425
- Neymark LA, Holm-Denoma CS, Larin AM, Moscatti RJ and Plotkina YV. 2021. LA-ICPMS U-Pb dating reveals cassiterite inheritance in the Yazov granite, Eastern Siberia; Implications for tin mineralization. *Mineralium Deposita*, 56(6): 1177–1194
- Olierook HKH, Rankenburg K, Ulrich S, Kirkland CL, Evans NJ, Brown S, McInnes BIA, Prent A, Gillespie J, McDonald B and Darragh M. 2020. Resolving multiple geological events using *in situ* Rb-Sr geochronology; Implications for metallogenesis at Tropicana, Western Australia. *Geochronology*, 2(2): 283–303
- Pfaff K, Romer RL and Markl G. 2009. U-Pb ages of ferberite, chalcedony, agate, 'U-mica' and pitchblende: Constraints on the mineralization history of the Schwarzwald ore district. *European Journal of Mineralogy*, 21(4): 817–836
- Poitrenaud T, Pujol M, Augier R and Marcoux E. 2020. The polyphase evolution of a Late Variscan W/Au deposit (Salau, French Pyrenees): Insights from REE and U/Pb LA-ICP-MS analyses. *Mineralium Deposita*, 55(6): 1127–1147
- Popov DV. 2022. Short communication: On the potential use of materials with heterogeneously distributed parent and daughter isotopes as primary standards for non-U-Pb geochronological applications of laser ablation inductively coupled plasma mass spectrometry (LA-ICP-MS). *Geochronology*, 4(1): 399–407
- Prokopyev IR, Doroshkevich AG, Starikova AE, Yang Y, Goryunova VO, Tomoshevich NA, Proskurnin VF, Saltanov VA and Kukharensko EA. 2023. Geochronology and origin of the carbonatites of the Central Taimyr Region, Russia (Arctica): Constraints on the F-Ba-REE mineralization and the Siberian Large Igneous Province. *Lithos*, 440–441: 107045
- Qin KZ, Zhao JX, He CT and Shi RZ. 2021. Discovery of the Qongjiagang giant lithium pegmatite deposit in Himalaya, Tibet, China. *Acta Petrologica Sinica*, 37(11): 3277–3286 (in Chinese with English abstract)
- Qu K, Sima XZ, Zhou HY, Xiao ZB, Tu JR, Yin QQ, Liu X and Li JH. 2019. *In situ* LA-MC-ICP-MS and ID-TIMS U-Pb ages of bastnäsite-(Ce) and zircon from the Taipingzheng hydrothermal REE deposit: New constraints on the Later Paleozoic granite-related U-REE mineralization in the North Qinling Orogen, Central China. *Journal of Asian Earth Sciences*, 173: 352–363
- Redaa A, Farkaš J, Gilbert S, Collins AS, Wade B, Löhr S, Zack T and Garbe-Schönberg D. 2021. Assessment of elemental fractionation and matrix effects during *in situ* Rb-Sr dating of phlogopite by LA-ICP-MS/MS; Implications for the accuracy and precision of mineral ages. *Journal of Analytical Atomic Spectrometry*, 36(2): 322–344
- Redaa A, Farkaš J, Hassan A, Collins AS, Gilbert S and Löhr SC. 2022. Constraints from *in-situ* Rb-Sr dating on the timing of tectono-thermal events in the Umm Farwah shear zone and associated Cu-Au mineralisation in the southern Arabian Shield, Saudi Arabia. *Journal of Asian Earth Sciences*, 224: 105037
- Redaa A, Farkaš J, Gilbert S, Collins AS, Löhr S, Vasegh D, Forster M, Blades M, Zack T, Giuliani A, Maas R, Baldermann A, Dietzel M and Garbe-Schönberg D. 2023. Testing nano-powder and fused-glass mineral reference materials for *in situ* Rb-Sr dating of glauconite, phlogopite, biotite and feldspar via LA-ICP-MS/MS. *Geostandards and Geoanalytical Research*, 47(1): 23–48
- Ribeiro BV, Kirkland CL, Kelsey DE, Reddy SM, Hartnady MIH, Faleiros FM, Rankenburg K, Liebmann J, Korhonen FJ and Clark C. 2023. Time-strain evolution of shear zones from petrographically constrained Rb-Sr muscovite analysis. *Earth and Planetary Science Letters*, 602: 117969
- Rizvanova NG and Kuznetsov AB. 2020. A new approach to ID-TIMS U-Pb dating of cassiterite by the example of the Pitkäranta tin deposit. *Doklady Earth Sciences*, 491(1): 146–149
- Romer RL and Wright JE. 1992. U-Pb dating of columbitites: A

- geochronologic tool to date magmatism and ore deposits. *Geochimica et Cosmochimica Acta*, 56(5): 2137–2142
- Romer RL and Smeds SA. 1994. Implications of U-Pb ages of columbite-tantalites from granitic pegmatites for the Palaeoproterozoic accretion of 1.90–1.85 Ga magmatic arcs to the Baltic Shield. *Precambrian Research*, 67(1–2): 141–158
- Romer RL and Lehmann B. 1995. U-Pb columbite age of Neoproterozoic Ta-Nb mineralization in Burundi. *Economic Geology*, 90(8): 2303–2309
- Romer RL and Smeds SA. 1996. U-Pb columbite ages of pegmatites from Sveconorwegian terranes in southwestern Sweden. *Precambrian Research*, 76(1–2): 15–30
- Romer RL, Smeds SA and Černý P. 1996. Crystal-chemical and genetic controls of U-Pb systematics of columbite-tantalite. *Mineralogy and Petrology*, 57(3–4): 243–260
- Romer RL and Smeds SA. 1997. U-Pb columbite chronology of post-kinematic Palaeoproterozoic pegmatites in Sweden. *Precambrian Research*, 82(1–2): 85–99
- Romer RL and Lüders V. 2006. Direct dating of hydrothermal W mineralization; U-Pb age for hübnerite (MnWO<sub>4</sub>), Sweet Home Mine, Colorado. *Geochimica et Cosmochimica Acta*, 70(18): 4725–4733
- Rösel D and Zack T. 2022. LA-ICP-MS/MS single-spot Rb-Sr dating. *Geostandards and Geoanalytical Research*, 46(2): 143–168
- Sal'nikova EB, Yakovleva SZ, Nikiforov AV, Kotov AB, Yarmolyuk VV, Anisimova IV, Sugorakova AM and Plotkina YV. 2010. Bastnaesite; A promising U-Pb geochronological tool. *Doklady Earth Sciences*, 430(1): 134–136
- Scanlan EJ, Scott JM, Wilson VJ, Stirling CH, Reid MR and Le Roux PJ. 2018. *In situ* <sup>87</sup>Sr/<sup>86</sup>Sr of scheelite and calcite reveals proximal and distal fluid-rock interaction during orogenic W-Au mineralization, Otago Schist, New Zealand. *Economic Geology*, 113(7): 1571–1586
- Scheibelhofer E, Moser U, Löhr S, Wilmsen M, Farkaš J, Gallhofer D, Bäckström AM, Zack T and Baldermann A. 2022. Revisiting glauconite geochronology: Lessons learned from *in situ* radiometric dating of a glauconite-rich Cretaceous Shelfal sequence. *Minerals*, 12(7): 818
- Schoene B, Crowley JL, Condon DJ, Schmitz MD and Bowring SA. 2006. Reassessing the uranium decay constants for geochronology using ID-TIMS U-Pb data. *Geochimica et Cosmochimica Acta*, 70(2): 426–445
- Şengün F, Erlandsson VB, Högmalin J and Zack T. 2019. *In situ* Rb-Sr dating of K-bearing minerals from the orogenic Akçaabat gold deposit in the Menderes Massif, Western Anatolia, Turkey. *Journal of Asian Earth Sciences*, 185: 104048
- Siebel W, Reitter E, Wenzel T and Blaha U. 2005. Sr isotope systematics of K-feldspars in plutonic rocks revealed by the Rb-Sr microdrilling technique. *Chemical Geology*, 222(3–4): 183–199
- Simpson A, Gilbert S, Tamblin R, Hand M, Spandler C, Gillespie J, Nixon A and Glorie S. 2021. *In-situ* Lu-Hf geochronology of garnet, apatite and xenotime by LA-ICP-MS/MS. *Chemical Geology*, 577: 120299
- Simpson A, Glorie S, Hand M, Spandler C, Gilbert S and Cave B. 2022. *In situ* Lu-Hf geochronology of calcite. *Geochronology*, 4(1): 353–372
- Simpson A, Glorie S, Hand M, Spandler C and Gilbert S. 2023. Garnet Lu-Hf speed dating: A novel method to rapidly resolve polymetamorphic histories. *Gondwana Research*, 121: 215–234
- Smith SR, Foster GL, Romer RL, Tindle AG, Kelley SP, Noble SR, Horstwood M and Breaks FW. 2004. U-Pb columbite-tantalite chronology of rare-element pegmatites using TIMS and laser ablation-multi collector-ICP-MS. *Contributions to Mineralogy and Petrology*, 147(5): 549–564
- Song GX, Cook NJ, Li GM, Qin KZ, Ciobanu CL, Yang YH and Xu YX. 2019. Scheelite geochemistry in porphyry-skarn W-Mo systems: A case study from the Gaojiabang deposit, East China. *Ore Geology Reviews*, 113: 103084
- Stern RA and Rayner N. 2003. Ages of several xenotime megacrysts by ID-TIMS: Potential reference materials for ion-microprobe U-Pb geochronology. Ontario: Natural Resources Canada
- Subarkah D, Blades ML, Collinš AS, Farkas J, Gilbert S, Löhr SC, Redaa A, Cassidy E and Zack T. 2022. Unraveling the histories of Proterozoic shales through *in situ* Rb-Sr dating and trace element laser ablation analysis. *Geology*, 50(1): 66–70
- Swart PK and Moore F. 1982. The occurrence of uranium in association with cassiterite, wolframite and sulphide mineralization in South-West England. *Mineralogical Magazine*, 46(339): 211–215
- Tamblin R, Hand M, Simpson A, Gilbert S, Wade B and Glorie S. 2022. *In situ* laser ablation Lu-Hf geochronology of garnet across the Western Gneiss Region: Campaign-style dating of metamorphism. *Journal of the Geological Society*, 179: jgs2021–094
- Tang Y, Zhao JY, Zhang H, Cai DW, Lv ZH, Liu YL and Zhang X. 2017. Precise columbite-(Fe) and zircon U-Pb dating of the Nanping No. 31 pegmatite vein in northeastern Cathaysia Block, SE China. *Ore Geology Reviews*, 83: 300–311
- Tang YW, Cui K, Zheng Z, Gao JF, Han JJ, Yang JH and Liu L. 2020. LA-ICP-MS U-Pb geochronology of wolframite by combining NIST series and common lead-bearing MTM as the primary reference material; Implications for metallogenesis of South China. *Gondwana Research*, 83: 217–231
- Tang YW, Han JJ, Lan TG, Gao JF, Liu L, Xiao CH and Yang JH. 2022. Two reliable calibration methods for accurate *in situ* U-Pb dating of scheelite. *Journal of Analytical Atomic Spectrometry*, 37(2): 358–368
- Tang ZM, Che XD, Yang YH, Wu FY, Wang RC, Yang JH, Gerdes A, Zhu ZY, Liu F and Zhang C. 2021. Precise and accurate Lu-Hf isotope analysis of columbite-group minerals by MC-ICP-MS. *Journal of Analytical Atomic Spectrometry*, 36(8): 1643–1656
- Tapster S and Bright JWG. 2020. High-precision ID-TIMS cassiterite U-Pb systematics using a low-contamination hydrothermal decomposition; Implications for LA-ICP-MS and ore deposit geochronology. *Geochronology*, 2(2): 425–441
- Tillberg M, Drake H, Zack T, Högmalin J and Åström M. 2017. *In situ* Rb-Sr dating of fine-grained vein mineralizations using LA-ICP-MS. *Procedia Earth and Planetary Science*, 17: 464–467
- Tillberg M, Drake H, Zack T, Kooijman E, Whitehouse MJ and Åström ME. 2020. *In situ* Rb-Sr dating of slickenfibres in deep crystalline basement faults. *Scientific Reports*, 10(1): 562
- Tu JR, Cui YR, Hao S, Li HM, Zhou HY and Geng JZ. 2016. An investigation of U-Pb isotope dating of cassiterite with isotope dilution-thermal ionization mass spectrometry. *Acta Geoscientia Sinica*, 37(6): 779–783 (in Chinese with English abstract)
- Tu JR, Xiao ZB, Qu K, Li GZ, Zhou HY, Li HM, Geng JZ, Cui YR, Hao S and Liu WG. 2017. A study of U-Pb dating technology of bastnaesite. *Acta Geoscientia Sinica*, 38(6): 945–951 (in Chinese with English abstract)
- Tu JR, Cui YR, Zhou HY, Li HM, Hao S and Li GZ. 2019. Review of U-Pb dating methods for cassiterite. *Geological Survey and Research*, 42(4): 241–249 (in Chinese with English abstract)
- Vasconcelos AD, Gonçalves GO, Lana C, Buick IS, Kamo SL, Corfu F, Scholz R, Alkmim A, Queiroga G and Nalini HA Jr. 2018. Characterization of xenotime from datas (Brazil) as a potential reference material for *in situ* U-Pb geochronology. *Geochemistry, Geophysics, Geosystems*, 19(7): 2262–2282
- Wang CY, Alard O, Lai YJ, Foley SF, Liu YS, Munnikhuis J and Wang Y. 2022. Advances in *in situ* Rb-Sr dating using LA-ICP-MS/MS: Applications to igneous rocks of all ages and to the identification of unrecognized metamorphic events. *Chemical Geology*, 610: 121073
- Wang H, Feng CY, Li RX, Li C, Zhao C, Chen X and Wang GH. 2021. Ore-forming mechanism and fluid evolution processes of the Xingluokeng tungsten deposit, western Fujian Province: Constraints from *in-situ* trace elemental and Sr isotopic analyses of scheelite. *Acta Petrologica Sinica*, 37(3): 698–716 (in Chinese with English abstract)
- Wang H, Yang YH and Yang JH. 2022. A review of progress in



- microbeam Lu-Hf isotopic analysis on mineral. *Rock and Mineral Analysis*, 41(6): 881–905 (in Chinese with English abstract)
- Wang RC, Wu FY, Xie L, Liu XC, Wang JM, Yang L, Lai W and Liu C. 2017. A preliminary study of rare-metal mineralization in the Himalayan leucogranite belts, South Tibet. *Science China (Earth Sciences)*, 60(9): 1655–1663
- Wang RC, Xie L, Zhu ZY and Hu H. 2019. Micas: Important indicators of granite-pegmatite-related rare-metal mineralization. *Acta Petrologica Sinica*, 35(1): 69–75 (in Chinese with English abstract)
- Wang RC, Che XD, Wu B and Xie L. 2020. Critical mineral resources of Nb, Ta, Zr and Hf in China. *Chinese Science Bulletin*, 65(33): 3763–3777 (in Chinese with English abstract)
- Wang RC, Wu B, Xie L, Che XD, Xiang L and Liu C. 2021. Global tempo-spatial distribution of rare-metal mineralization and continental evolution. *Acta Geologica Sinica*, 95(1): 182–193 (in Chinese with English abstract)
- Wang W, Zhou MZ, Chu ZY, Xu JJ, Li CF, Luo TY and Guo JH. 2020. Constraints on the Ediacaran-Cambrian boundary in deep-water realm in South China: Evidence from zircon CA-ID-TIMS U-Pb ages from the topmost Liuchapo Formation. *Science China (Earth Sciences)*, 63(8): 1176–1187
- Wang ZQ, Li C, Zhang DC, Jiang XJ, Zhou LM and Yan QG. 2020. Implication of *in situ* Sr isotope of scheelite for tungsten mineralization: A case study of the Nanyangian scheelite deposit, Southeast Yunnan, China. *Rock and Mineral Analysis*, 39(2): 285–299 (in Chinese with English abstract)
- Wei GJ, Huang F, Ma JL, Deng WF, Yu HM, Kang JT and Chen XF. 2022. Progress of non-traditional stable isotope geochemistry of the past decade in China. *Bulletin of Mineralogy, Petrology and Geochemistry*, 41(1): 1–44 (in Chinese with English abstract)
- Wei QD, Yang M, Romer RL, Wang H, Yang YH, Zhao ZF, Wu ST, Xie LW, Huang C, Xu L, Yang JH and Wu FY. 2022. *In situ* U-Pb geochronology of vesuvianite by LA-SF-ICP-MS. *Journal of Analytical Atomic Spectrometry*, 37(1): 69–81
- Wintzer NE, Gillerman VS and Schmitz MD. 2016. Eocene U-Pb scheelite LA-ICP-MS dates of stibnite-scheelite mineralization in the Yellow Pine Au-Sb-W mining area, Central Idaho, USA. In: *GSA Annual Meeting*. Denver: GSA
- Wintzer NE, Schmitz MD, Gillerman VS and Vervoot JD. 2022. U-Pb scheelite ages of tungsten and antimony mineralization in the stibnite, Yellow Pine district, Central Idaho. *Economic Geology*, doi: 10.5382/econgeo.4953
- Wu CZ, Jia L, Lei RX, Chen BY, Feng ZJ, Feng YG, Zhi J and Bai SH. 2021. Advances and general characteristics of the amazonite granite and related rubidium deposits in Central Asian Orogenic Belt. *Acta Petrologica Sinica*, 37(9): 2604–2628 (in Chinese with English abstract)
- Wu FY, Li XH, Zheng YF and Gao S. 2007. Lu-Hf isotopic systematics and their applications in petrology. *Acta Petrologica Sinica*, 23(2): 185–220 (in Chinese with English abstract)
- Wu FY, Liu XC, Ji WQ, Wang JM and Yang L. 2017. Highly fractionated granites: Recognition and research. *Science China (Earth Sciences)*, 60(7): 1201–1219
- Wu FY, Wang RC, Liu XC and Xie L. 2021. New breakthroughs in the studies of Himalayan rare-metal mineralization. *Acta Petrologica Sinica*, 37(11): 3261–3276 (in Chinese with English abstract)
- Wu FY, Guo CL, Hu FY, Liu XC, Zhao JX, Li XF and Qin KZ. 2023. Petrogenesis of the highly fractionated granites and their mineralizations in Nanling Range, South China. *Acta Petrologica Sinica*, 39(1): 1–36 (in Chinese with English abstract)
- Wu KY, Liu B, Wu QH, Chen SF, Kong H, Li H and Elatikpo SM. 2023. Trace element geochemistry, oxygen isotope and U-Pb geochronology of multistage scheelite: Implications for W-mineralization and fluid evolution of Shizhuyuan W-Sn deposit, South China. *Journal of Geochemical Exploration*, 248: 107192
- Wu ST, Yang M, Yang YH, Xie LW, Huang C, Wang H and Yang JH. 2020. Improved *in situ* zircon U-Pb dating at high spatial resolution (5–16 μm) by laser ablation-single collector-sector field-ICP-MS using Jet sample and X skimmer cones. *International Journal of Mass Spectrometry*, 456: 116394
- Wu ST, Yang YH, Roberts NMW, Yang M, Wang H, Lan ZW, Xie BH, Li TY, Xu L, Huang C, Xie LW, Yang JH and Wu FY. 2022. *In situ* calcite U-Pb geochronology by high-sensitivity single-collector LA-SF-ICP-MS. *Science China (Earth Sciences)*, 65(6): 1146–1160
- Xiang DF, Zhang ZY, Zack T, Chew D, Yang YH, Wu L and Hogmalm J. 2021. Apatite U-Pb dating with common Pb correction using LA-ICP-MS/MS. *Geostandards and Geoanalytical Research*, 45(4): 621–642
- Xiang L, Wang RC, Romer RL, Che XD, Hu H and Tang ZM. 2023. Columbite Sn3: A new potential reference material for U-Pb dating by LA-ICP-MS. *Geostandards and Geoanalytical Research*, 47(3): 609–628
- Xie BH, Wu ST, Yang YH, Wang H, Zhao ZF, Huang C and Xie LW. 2023. LA-MC-ICP-MS calcite U-Pb dating technique. *Acta Petrologica Sinica*, 39(1): 236–248 (in Chinese with English abstract)
- Xu L, Hu ZC, Zhang W, Yang L, Liu YS, Gao S, Luo T and Hu SH. 2015. *In situ* Nd isotope analyses in geological materials with signal enhancement and non-linear mass dependent fractionation reduction using laser ablation MC-ICP-MS. *Journal of Analytical Atomic Spectrometry*, 30(1): 232–244
- Xu L, Yang JH, Ni Q, Yang YH, Hu ZC, Liu YS, Wu YB, Luo T and Hu SH. 2018. Determination of Sm-Nd isotopic compositions in fifteen geological materials using laser ablation MC-ICP-MS and application to monazite geochronology of metasedimentary rock in the North China Craton. *Geostandards and Geoanalytical Research*, 42(3): 379–394
- Xu ZQ, Zhu WB, Zheng BH, Shu LS, Li GW, Che XD and Qin YL. 2021. New energy strategy for lithium resource and the continental dynamics research: Celebrating the centenary of the School of Earth Sciences and Engineering, Nanjing University. *Acta Geologica Sinica*, 95(10): 2937–2954 (in Chinese with English abstract)
- Yang M, Yang YH, Wu ST, Romer RL, Che XD, Zhao ZF, Li WS, Yang JH, Wu FY, Xie LW, Huang C, Zhang D and Zhang Y. 2020. Accurate and precise *in situ* U-Pb isotope dating of wolframite series minerals via LA-SF-ICP-MS. *Journal of Analytical Atomic Spectrometry*, 35(10): 2191–2203
- Yang M, Wang H, Wu ST and Yang YH. 2021. Research progress of geochemistry in tungsten deposit: Based on the Wolframite U-Pb, Sm-Nd, Lu-Hf isotope geochronology and trace element characteristics. *Geological Journal of China Universities*, 27(3): 249–263 (in Chinese with English abstract)
- Yang M. 2022. *In situ* U-Pb geochronology of tungsten and tin ore minerals and its application. Ph. D. Dissertation. Beijing: Institute of Geology and Geophysics, Chinese Academy of Sciences (in Chinese with English abstract)
- Yang M, Romer RL, Yang YH, Wu ST, Wang H, Tu JR, Zhou HY, Xie LW, Huang C, Xu L, Yang JH and Wu FY. 2022a. U-Pb isotopic dating of cassiterite: Development of reference materials and *in situ* applications by LA-SF-ICP-MS. *Chemical Geology*, 593: 120754
- Yang M, Yang YH, Kamo SL, Romer RL, Roberts NMW, Wang H, Xie LW, Huang C, Yang JH and Wu FY. 2022b. Natural allanite reference materials for *in situ* U-Th-Pb and Sm-Nd isotopic measurements by LA-(MC)-ICP-MS. *Geostandards and Geoanalytical Research*, 46(2): 169–203
- Yang M, Yang YH, Romer RL, Wu ST, Wu T and Wang H. 2023a. *In situ* Hf isotope analysis of cassiterite by LA-MC-ICP-MS: Protocol and applications. *Journal of Analytical Atomic Spectrometry*, 38(2): 437–448
- Yang M, Yang YH, Romer RL, Che XD, Wang RC, Wu FY, Fei GC, Deng Y and Wu T. 2023b. Characterization of reference materials for *in situ* U-Pb dating of columbite group minerals by LA-ICP-MS. *Journal of Analytical Atomic Spectrometry*, 38(9): 1816–1829

Yang YH, Sun JF, Xie LW, Fan HR and Wu FY. 2008. *In situ* Nd isotopic measurement of natural geological materials by LA-MC-ICPMS. *Science Bulletin*, 53(7): 1062–1070

Yang YH, Wu FY, Wilde SA, Liu XM, Zhang YB, Xie LW and Yang JH. 2009. *In situ* perovskite Sr-Nd isotopic constraints on the petrogenesis of the Ordovician Mengyin kimberlites in the North China Craton. *Chemical Geology*, 264(1–4): 24–42

Yang YH, Wu FY, Yang JH, Chew DM, Xie LW, Chu ZY, Zhang YB and Huang C. 2014. Sr and Nd isotopic compositions of apatite reference materials used in U-Th-Pb geochronology. *Chemical Geology*, 385: 35–55

Yang YH, Wu FY, Li QL, Rojas-Agramonte Y, Yang JH, Li Y, Ma Q, Xie LW, Huang C, Fan HR, Zhao ZF and Xu C. 2019. *In situ* U-Th-Pb dating and Sr-Nd isotope analysis of bastnäsite by LA-(MC)-ICP-MS. *Geostandards and Geoanalytical Research*, 43(4): 543–565

Yang YH, Yang M, Wang H, Yang JH and Wu FY. 2021. Methodology for *in situ* wolframite U-Pb dating and its application. *Science China (Earth Sciences)*, 64(1): 187–190

Yuan SD, Peng JT, Hu RZ, Li HM, Shen NP and Zhang DL. 2008. A precise U-Pb age on cassiterite from the Xianghualing tin-polymetallic deposit (Hunan, South China). *Mineralium Deposita*, 43(4): 375–382

Yuan SD, Peng JT, Hao S, Li HM, Geng JZ and Zhang DL. 2011. *In situ* LA-MC-ICP-MS and ID-TIMS U-Pb geochronology of cassiterite in the giant Furong tin deposit, Hunan Province, South China: New constraints on the timing of tin – polymetallic mineralization. *Ore Geology Reviews*, 43(1): 235–242

Zack T and Hogmalm J. 2015. In-situ Lu-Hf dating of xenotime by reaction cell isotope separation. Prague, Czech Republic: Goldschmidt, 3557

Zack T and Hogmalm KJ. 2016. Laser ablation Rb/Sr dating by online chemical separation of Rb and Sr in an oxygen-filled reaction cell. *Chemical Geology*, 437: 120–133

Zhai MG, Wu FY, Hu RZ, Jiang SY, Li WC, Wang RC, Wang DH, Qi T, Qin KZ and Wen HJ. 2019. Critical metal mineral resources: Current research status and scientific issues. *Bulletin of National Natural Science Foundation of China*, 33(2): 106–111 (in Chinese with English abstract)

Zhang DL, Peng JT, Hu RZ, Yuan SD and Zheng DS. 2011. The closure of U-Pb isotope system in cassiterite and its reliability for dating. *Geological Review*, 57(4): 549–554 (in Chinese with English abstract)

Zhang DL, Peng JT, Coulson IM, Hou LH and Li SJ. 2014. Cassiterite U-Pb and muscovite  $^{40}\text{Ar}$ - $^{39}\text{Ar}$  age constraints on the timing of mineralization in the Xuebaoding Sn-W-Be deposit, western China. *Ore Geology Reviews*, 62: 315–322

Zhang LL, Zhu DC, Yang YH, Wang Q, Xie JC and Zhao ZD. 2021. U-Pb geochronology of carbonate by laser ablation MC-ICP-MS: Method improvements and geological applications. *Atomic Spectroscopy*, 42(6): 335–348

Zhang RQ, Lu JJ, Wang RC, Yang P, Zhu JC, Yao Y, Gao JF, Li C, Lei ZH, Zhang WL and Guo WM. 2015. Constraints of *in situ* zircon and cassiterite U – Pb, molybdenite Re-Os and muscovite  $^{40}\text{Ar}$ - $^{39}\text{Ar}$  ages on multiple generations of granitic magmatism and related W-Sn mineralization in the Wangxianling area, Nanling Range, South China. *Ore Geology Reviews*, 65: 1021–1042

Zhang RQ, Lu JJ, Lehmann B, Li CY, Li GL, Zhang LP, Guo J and Sun WD. 2017a. Combined zircon and cassiterite U-Pb dating of the Piaotang granite-related tungsten-tin deposit, southern Jiangxi tungsten district, China. *Ore Geology Reviews*, 82: 268–284

Zhang RQ, Lehmann B, Seltmann R, Sun WD and Li CY. 2017b. Cassiterite U-Pb geochronology constrains magmatic-hydrothermal evolution in complex evolved granite systems: The classic Erzgebirge tin province (Saxony and Bohemia). *Geology*, 45(12): 1095–1098

## 附中文参考文献

陈靖, 侯可军, 王倩, 袁顺达, 陈岳龙. 2021. 非基体匹配分馏校正的 LA-ICP-MS 锡石微区 U-Pb 定年方法研究. *岩石学报*, 37(3): 943–955

储著银, 许俊杰, 陈知, 李潮峰, 李向辉, 贺怀宇, 李献华, 郭敬辉. 2016. 超低本底单颗粒锆石 CA-ID-TIMS U-Pb 高精度定年方法. *科学通报*, 61(10): 1121–1129

崔玉荣, 涂家润, 陈枫, 郝爽, 叶丽娟, 周红英, 李惠民. 2017. LA-(MC)-ICP-MS 锡石 U-Pb 定年研究进展. *地质学报*, 91(6): 1386–1399

郝爽, 李惠民, 李国占, 耿建珍, 周红英, 肖志斌, 崔玉荣, 涂家润. 2016. LA-ICP-MS 测定锡石 U-Pb 同位素年龄时两种普通铅扣除方法的原理及适用性比较. *地质通报*, 35(4): 622–632

侯可军, 秦燕, 李延河, 范昌福. 2013. 磷灰石 Sr-Nd 同位素的激光剥蚀-多接收器电感耦合等离子体质谱微区分析. *岩矿测试*, 32(4): 547–554

黄超, 王浩, 师文贝, 孙金凤, 胡方泱, 许蕾, 杨岳衡, 吴石头, 谢烈文, 杨进辉. 2023. 云母 Rb-Sr 等时线年龄原位微区 LA-ICP-MS/MS 测定. *中国科学(地球科学)*, 53(11): 2648–2668

蒋少涌, 赵葵东, 姜海, 苏慧敏, 熊索非, 熊伊曲, 徐耀明, 章伟, 朱律运. 2020. 中国钨锡矿床时空分布规律、地质特征与成矿机制研究进展. *科学通报*, 65(33): 3730–3745

蒋少涌, 王春龙, 张璐, 袁峰, 苏慧敏, 张浩翔, 刘涛. 2021. 伟晶岩型锂矿中矿物原位微区元素和同位素示踪与定年研究进展. *地质学报*, 95(10): 3017–3038

李建康, 李鹏, 严清高, 王登红, 任广利, 丁欣. 2023. 松潘-甘孜-西昆仑花岗伟晶岩型稀有金属成矿带成矿规律. *中国科学(地球科学)*, 53(8): 1718–1740

李杨, 杨岳衡, 焦淑娟, 吴福元, 杨进辉, 谢烈文, 黄超. 2016. 金红石 Hf 同位素激光原位多接收等离子体质谱 (LA-MC-ICP-MS) 测定. *中国科学(地球科学)*, 46(6): 857–869

刘玉平, 李正祥, 李惠民, 郭利果, 徐伟, 叶霖, 李朝阳, 皮道会. 2007. 都龙锡锌矿床锡石和锆石 U-Pb 年代学: 滇东南白垩纪大规模花岗岩成岩-成矿事件. *岩石学报*, 23(5): 967–976

刘志超, 吴福元, 郭春丽, 赵子福, 杨进辉, 孙金凤. 2011. 磷钇矿 U-Pb 年龄激光原位 ICP-MS 测定. *科学通报*, 56(33): 2772–2781

罗涛, 赵赫, 张文, 郭京梁, 宗克清, 刘勇胜, 章军锋, 胡兆初. 2021. 激光剥蚀电感耦合等离子体质谱非基体匹配配氟铈矿 U-Th-Pb 定年. *中国科学(地球科学)*, 51(6): 874–883

罗涛, 胡兆初. 2022. 激光剥蚀电感耦合等离子体质谱副矿物 U-Th-Pb 定年新进展. *地球科学*, 47(11): 4122–4144

毛景文, 吴胜华, 宋世伟, 戴盼, 谢桂青, 苏蔷薇, 刘鹏, 王先广, 余忠珍, 陈祥云, 唐维新. 2020. 江南世界级钨矿带: 地质特征、成矿规律和矿床模型. *科学通报*, 65(33): 3746–3762

秦克章, 赵俊兴, 何畅通, 施睿哲. 2021. 喜马拉雅琼嘉岗超大型伟晶岩型锂矿的发现及意义. *岩石学报*, 37(11): 3277–3286

涂家润, 崔玉荣, 郝爽, 李惠民, 周红英, 耿建珍. 2016. 同位素稀释热电离质谱法测定锡石 U-Pb 年龄探索. *地球学报*, 37(6): 779–783

- 涂家润, 肖志斌, 曲凯, 李国占, 周红英, 李惠民, 耿建珍, 崔玉荣, 郝爽, 刘文刚. 2017. 氟碳铈矿 U-Pb 定年技术研究. 地球学报, 38(6): 945-951
- 涂家润, 崔玉荣, 周红英, 李惠民, 郝爽, 李国占. 2019. 锡石 U-Pb 定年方法评述. 地质调查与研究, 42(4): 241-249
- 王辉, 丰成友, 李荣西, 李超, 赵超, 陈欣, 王光华. 2021. 闽西行洛坑钨矿流体演化过程与成矿机制: 白钨矿原位微量元素、Sr 同位素的制约. 岩石学报, 37(3): 698-716
- 王浩, 杨岳衡, 杨进辉. 2022. 矿物微区 Lu-Hf 同位素分析技术研究进展. 岩矿测试, 41(6): 881-905
- 王汝成, 吴福元, 谢磊, 刘小驰, 王佳敏, 杨雷, 赖文, 刘晨. 2017. 藏南喜马拉雅淡色花岗岩稀有金属成矿作用初步研究. 中国科学(地球科学), 47(8): 871-880
- 王汝成, 谢磊, 诸泽颖, 胡欢. 2019. 云母: 花岗岩-伟晶岩稀有金属成矿作用的重要标志矿物. 岩石学报, 35(1): 69-75
- 王汝成, 车旭东, 邬斌, 谢磊. 2020. 中国铈钨钨钨资源. 科学通报, 65(33): 3763-3777
- 王汝成, 邬斌, 谢磊, 车旭东, 向路, 刘晨. 2021. 稀有金属成矿全球时空分布与大陆演化. 地质学报, 95(1): 182-193
- 王伟, 周明忠, 储著银, 许俊杰, 李潮峰, 罗泰义, 郭敬辉. 2020. 华南深水区域埃迪卡拉系-寒武系界线制约: 来自留茶坡组顶部锆石 CA-ID-TIMS U-Pb 年龄证据. 中国科学(地球科学), 50(6): 819-831
- 王忠强, 李超, 张定才, 江小均, 周利敏, 严清高. 2020. 滇东南南秧田钨矿床白钨矿原位 Sr 同位素对成矿的指示. 岩矿测试, 39(2): 285-299
- 韦刚健, 黄方, 马金龙, 邓文峰, 于慧敏, 康晋霆, 陈雪霏. 2022. 近十年我国非传统稳定同位素地球化学研究进展. 矿物岩石地球化学通报, 41(1): 1-44
- 吴昌志, 贾力, 雷如雄, 陈博洋, 丰志杰, 凤永刚, 智俊, 白世恒. 2021. 中亚造山带天河石花岗岩及相关钨矿床的主要特征与研究进展. 岩石学报, 37(9): 2604-2628
- 吴福元, 李献华, 郑永飞, 高山. 2007. Lu-Hf 同位素体系及其岩石学应用. 岩石学报, 23(2): 185-220
- 吴福元, 刘小驰, 纪伟强, 王佳敏, 杨雷. 2017. 高分异花岗岩的识别与研究. 中国科学(地球科学), 47(7): 745-765
- 吴福元, 王汝成, 刘小驰, 谢磊. 2021. 喜马拉雅稀有金属成矿作用研究的新突破. 岩石学报, 37(11): 3261-3276
- 吴福元, 郭春丽, 胡方泱, 刘小驰, 赵俊兴, 李晓峰, 秦克章. 2023. 南岭高分异花岗岩成岩与成矿. 岩石学报, 39(1): 1-36
- 吴石头, 杨岳衡, Roberts NMW, 杨明, 王浩, 兰中伍, 谢博航, 李天义, 许蕾, 黄超, 谢烈文, 杨进辉, 吴福元. 2022. 高灵敏度-单接收杯 LA-SF-ICP-MS 原位方解石 U-Pb 定年. 中国科学(地球科学), 52(7): 1375-1390
- 谢博航, 吴石头, 杨岳衡, 王浩, 赵子福, 黄超, 谢烈文. 2023. LA-MC-ICP-MS 方解石 U-Pb 定年技术. 岩石学报, 39(1): 236-248
- 许志琴, 朱文斌, 郑碧海, 舒良树, 李广伟, 车旭东, 秦宇龙. 2021. 新能源锂电战略与大陆动力学研究——纪念南京大学地球科学与工程学院 100 周年华诞. 地质学报, 95(10): 2937-2954
- 杨明, 王浩, 吴石头, 杨岳衡. 2021. 钨矿床地球化学研究进展: 以黑钨矿 U-Pb、Sm-Nd、Lu-Hf 同位素年代学与微量元素为例. 高校地质学报, 27(3): 249-263
- 杨明. 2022. 钨锡矿石矿物激光微区 U-Pb 年代学方法及应用. 博士学位论文. 北京: 中国科学院地质与地球物理研究所
- 杨岳衡, 杨明, 王浩, 杨进辉, 吴福元. 2021. 微区原位黑钨矿 U-Pb 年代学方法及应用. 中国科学(地球科学), 51(1): 171-174
- 翟明国, 吴福元, 胡瑞忠, 蒋少涌, 李文昌, 王汝成, 王登红, 齐涛, 秦克章, 温汉捷. 2019. 战略性关键金属矿产资源: 现状与问题. 中国科学基金, 33(2): 106-111
- 张东亮, 彭建堂, 胡瑞忠, 袁顺达, 郑德顺. 2011. 锡石 U-Pb 同位素体系的封闭性及其测年的可靠性分析. 地质论评, 57(4): 549-554